THE RELATIONSHIP BETWEEN INCOMING SOLAR RADIATION AND DAILY AIR TEMPERATURE

DANIEL KWASI KPEGLO

10357537

THIS THESIS IS SUBMITTED TO THE UNIVERSITY OF GHANA, LEGON IN PARTIAL FULFILLMENT OF THE REQUIREMENT FOR THE AWARD OF MPHIL PHYSICS DEGREE

JUNE 2013

DECLARATION

This thesis is the result of research work undertaken by Daniel Kwasi Kpeglo for my Mphil degree in the Department of Physics, University of Ghana, under the supervision of Dr. V.C.K. Kakane and Dr. Michael Addae-Kagyah.

References made to other research works and publications are duly cited within the text.

This thesis has not, either in part or in its entirety, been published elsewhere, nor has it been offered for the award of another degree.

Sign ……..

Daniel Kwasi Kpeglo

(STUDENT)

Sign……

Dr. V. C. K. Kakane

(SUPERVISOR)

Sign …….

Dr. Michael Addae-Kagyah

(SUPERVISOR)

DEDICATION

To my father Mr. James Peter Kpeglo, who has been there for me through thick and thin. He is my biggest pride and secondly to Mrs. Comfort Setordzi of blessed memory.

ACKNOWLEDGEMENT

My utmost thanks go to the Almighty God, the creator of the universe for giving me the strength, courage and direction to make this work a success.

I am also grateful for the excellent supervision provided by Dr. V. C. K. Kakane and Dr. Michael Addae-Kaygyah. I pray that God renews their strength, wisdom, restore and increase their knowledge they imparted in me.

I am also indebted to Mr. Kofi Azoda for willingly making his equipment and laboratory available for me during this work. God richly bless him.

I wish to take this opportunity to thank the entire teaching staff of the Physics Department for the wonderful work they are doing.

I wish to say a very big thank you to Ms. Elizabeth Afia Acheampong, Ms. Golda Elorm Kudalor, and Ms. Joyce Ama Kpeglo for the encouragement, support and prayers during this work. May God reward them according to His riches in glory.

To the technicians of the Physics Department of the University of Ghana, God bless them all in their endeavors.

Last but definitely not the least, I want to express my thanks to my friends and colleagues for their immense support.

ABSTRACT

Solar radiation is the ultimate source of energy for the planet. To predict the values of temperature and instant solar radiation when equipment are not readily available from obtained equations, a good knowledge and understanding of the disposition and distribution of solar radiation is a requirement for modelling earth's weather and climate change variables. A pyranometer (CM3) in series with a PHYWE amplifier and a voltmeter were experimentally set-up and used to study the amount of solar radiation received at the Physics Department of the University of Ghana during the day. The temperature of the study area as well as the Relative Humidity was also recorded. Data was collected over a period of one month (from 2nd to 24th April, 2012). Days for which rain was recorded were ignored because rain could damage the pyranometer. The data obtained by the set-up were therefore used to compare with data obtained by a wireless weather station (Davis Vintage Pro). The data from these separate set-ups indicated that a perfect correlation existed between the solar radiation and temperature of the place. The data obtained by the experimental set-up was split into two separate sessions as morning and evening sessions. It was observed that the experimental set-up had a good correlation with that of the weather station on a particular day 11th April, 2012. The various Regression Coefficient (R^2) values for morning session were respectively $R^2 = 0.96$ and $R^2 = 0.95$ with their respective equations as $I_W = 136.22T_W - 40623$ and $I_p = 2.3198T_P - 678.14$. The evening session also had good Regression Coefficient values of $R^2 = 0.81\ and\ R^2 = 0.97$ with equations of $I_P = 2.1098T_P - 625$ and $I_W = 161.31T_W - 48769$. Similar analysis of the data from the separate set-ups gave a better correlation for that of the experimental set-up than that of the wireless station. The range of values of Regression Coefficient (R^2) for the experimental set-up was between $0.82 - 0.99$ for the morning and $0.45 - 0.98$ for the evening while the wireless station had $0.10 - 0.95$ for the morning and

$0.18 - 0.98$ for the evening sessions. Analysis performed on the data set for the entire period indicated that a strong correlation existed between the mean solar radiation (I_m) and the mean temperature (T_m). The equations obtained for both set-ups for the morning and evening sessions were found to be; $I_m = 2.417T_m - 713$ with a Regression Coefficient (R^2) value of 0.98 and $I_m = 3.265T_m - 974$ with a Regression Coefficient (R^2) value of 0.97.

TABLE OF CONTENTS

DECLARATION i
DEDICATION ii
ACKNOWLEDGEMENT iii
ABSTRACT iv
LIST OF FIGURES viii
LIST OF TABLES xv

CHAPTER ONE 1
1.0 Introduction 1
1.1 Composition of the atmosphere 2
1.2 Atmospheric structure and temperature 4
1.3 The climatic regions of Ghana 7
1.4 Solar radiative transfer 9
1.5 Measurement of solar radiation 10
1.6 Instruments used in measuring solar radiation 13
1.7 Objectives of this work 15
1.8 The study area 15
1.9 Motivation for the study 15
1.10 Literature review 16

CHAPTER TWO 21
THEORY 21
2.0 Nature of Electromagnetic radiation 21
2.1 Blackbody radiation and the radiation laws 21
2.2 The cosine law of emission and absorption 23
2.3 The Pyranometer and its theory of operation 25

CHAPTER THREE 27
METHODOLOGY 27
3.0 Measurement of meteorological parameters 27
3.1 Experimental set-up 28

3.2 Data acquisition using the automatic wireless weather station 30
3.3 Data collection: measuring solar radiation, temperature and relative humidity..... 32
3.4 Data collection using the experimental set-up..... 33
3.5 Analysis of the data collected..... 34

CHAPTER FOUR..... 35
RESULTS AND DISCUSSION 35
4.0 Introduction 35
4.1 Diurnal relationship between temperature and solar radiation with time..... 35
4.2 Empirical relationships between solar radiation and temperature..... 40
4.3 Correlation between the experimental set-up and the wireless weather station 69
4.4 Correlation between the mean solar radiation (Im) against mean temperature (Tm)..... 70
4.5 Comparing this work with other related works 72

CHAPTER FIVE 73
5.0 CONCLUSION AND SUMMARY..... 73
5.1 RECOMMENDATIONS 75
REFFERENCES 76

LIST OF FIGURES

Fig. 1.1: Detailed diagram of the electromagnetic spectrum. Adapted from Wikipedia, 2012……..1

Fig. 1.2: Layers of the atmosphere as related to the average profile of air temperature above the Earth's surface. The heavy line illustrates how the average temperature varies in each layer. Adapted from Ahrens, 2006…….5

Fig. 1.3: Map showing the intercontinental convergence zone describing the prevailing winds necessary for the two main seasons in the country (Adapted from Ghana Meteorological Agency, 2002)……8

Fig. 1.4: Interactions associated with the absorption and distribution of solar radiation on the Biosphere. Adapted from Fundamentals of Physical Geography……..10

Fig. 1.5: Extraterrestrial solar spectrum. Adapted from Geymard, 2004...……..11

Fig. 1.6: Distribution of the solar radiation components. Adapted from Stoffel and Wilcox, 2004.

……13

Fig. 1.7: Pyranometer for measuring global horizontal radiation. (Adapted from Stoffel and Wilcox, 2004)……14

Fig. 2.1: The amount of radiation intercepted by a radiometer from the surface XY is independent of the angle of emission, but the flux emitted per unit area is proportional to $cos\theta$. Adapted from Monteith, 1973……24

Fig. 2.2: Construction details of a Pyranometer. Adapted from Kipp and Zonen instruction manual, 2004……25

Fig. 3.1: Diagram showing the different equipment used for data collection at the Department of Physics, Legon……...28

Fig. 3.2: Davis Wireless Weather Station: Vintage Pro2 Plus. Adapted from Davis Instruments, Davis, CA, USA……30

Fig. 3.3: Picture of a mounted Davis Wireless Weather Station at the Department of Physics, Legon……31

Fig. 4.1: Solar radiation and Temperature recorded on the University of Ghana campus on April 2, 2012……37

Fig. 4.2: Solar radiation and Temperature recorded on the University of Ghana campus on April 3, 2012……37

Fig. 4.3: Solar radiation and Temperature recorded on the University of Ghana campus on April 4, 2012……38

Fig. 4.4: Solar radiation and Temperature recorded on the University of Ghana campus on April 5, 2012……38

Fig. 4.5: Solar radiation and Temperature recorded on the University of Ghana campus on April 6, 2012……39

Fig. 4.6: Solar radiation and temperature recorded on the University of Ghana campus on April 11, 2012……39

Fig. 4.7: Solar radiation and Temperature recorded on the University of Ghana campus on April 12, 2012……..40

Fig. 4.8: Linear regression analysis of solar radiation (I_p) against temperature (T_p) for the morning session for the experimental set-up recorded on April 2, 2012……...42

Fig. 4.9: Linear regression analysis of solar radiation (I_w) against temperature (T_w) for the morning session for the wireless weather station recorded on April 2, 2012……42

Fig. 4.10: Linear regression analysis of solar radiation (I_p) against temperature (T_p) for the evening session for the experimental set-up recorded on April 2, 2012……43

Fig. 4.11: Linear regression analysis of solar radiation (I_w) against temperature (T_w) for the evening session for the wireless weather station recorded on April 2, 2012……43

Fig. 4.12: Linear regression analysis of solar radiation (I_p) against temperature (T_p) for the morning session for the experimental set-up recorded on April 3, 2012……...44

Fig. 4.13: Linear regression analysis of solar radiation (I_w) against temperature (T_w) for the morning session for the wireless weather station recorded on April 3, 2012……44

Fig. 4.14: Linear regression analysis of solar radiation (I_p)against temperature (T_p)for the evening session for the experimental set-up recorded on April 3, 2012……45

Fig. 4.15: Linear regression analysis of solar radiation (I_w) against temperature (T_w) for the evening session for the weather station recorded on April 3, 2012……...45

Fig. 4.16: Linear regression analysis of solar radiation (I_p) against temperature (T_p) for the morning session for the experimental set-up recorded on April 4, 2012……...46

Fig. 4.17: Linear regression analysis of solar radiation (I_w) against temperature (T_w)for the morning session for the wireless weather station recorded on April 4, 2012……47

Fig 4.18: Linear regression analysis of solar radiation (I_p) against temperature (T_p) for the evening session for the experimental set-up recorded on April 4, 2012……47

Fig. 4.19: Linear regression analysis of solar radiation (I_w) against temperature (T_w)for the evening session for the wireless weather station recorded on April 4, 2012……48

Fig. 4.20: Linear regression analysis of solar radiation (I_p)against temperature (T_p)for the morning session the experimental set-up recorded on April 5, 2012……48

Fig. 4.21: Linear regression analysis of solar radiation (I_w) against temperature (T_w) for the morning session for the wireless weather station recorded on April 5, 2012……49

Fig. 4.22: Linear regression analysis of solar radiation (I_p) against temperature (T_p) for the evening session for the experimental set-up recorded on April 5, 2012…….....49

Fig. 4.23: Linear regression analysis of solar radiation (I_w) against temperature (T_w) for the evening session for the wireless weather station recorded on April 5, 2012……50

Fig 4.24: Linear regression analysis of solar radiation (I_p)against temperature (T_p)for the morning session for the experimental set-up recorded on April 6, 2012……...50

Fig. 4.25: Linear regression analysis of solar radiation (I_w) against temperature (T_w) for the morning session for wireless weather station recorded on April 6, 2012……..51

Fig. 4.26: Linear regression analysis of solar radiation (I_p)against temperature (T_p) for the evening session for the experimental set-up recorded on April 6, 2012……..51

Fig. 4.27: Linear regression analysis of solar radiation (I_w) against temperature (T_w) for the evening session for the wireless weather station recorded on April 6, 2012……52

Fig. 4.28: Linear regression analysis for solar radiation (I_p) against temperature (T_p) for the morning session for the experimental set-up recorded on April 11, 2012……52

Fig. 4.29: Linear regression analysis for solar radiation (I_w) against temperature (T_w)for the morning session for the wireless weather station recorded on April 11, 2012……..53

Fig. 4.30: Linear regression analysis for solar radiation (I_p) against temperature (T_p) for the evening session for the experimental set-up recorded on April 11, 2012……..53

Fig. 4.31: Linear regression analysis for solar radiation (I_w) against temperature (T_w) for the evening session for the wireless weather station recorded on April 11, 2012……...54

Fig. 4.32: Linear regression analysis of solar radiation (I_p) against temperature (T_p) for the morning session for the experimental set-up recorded on April 12, 2012……54

Fig. 4.33: Linear regression analysis of solar radiation (I_w) against temperature (T_w) for the morning session for the wireless weather station recorded on April 12, 2012……..55

Fig. 4.34: Linear regression analysis of solar radiation (I_p) against temperature (T_p) for the evening session for the experimental set-up recorded on April 12, 2012……..55

Fig. 4.35: Linear regression analysis of solar radiation (I_w) against temperature (T_w) for the evening session for the wireless weather station recorded on April 12, 2012……...56

Fig. 4.36: Linear regression analysis of solar radiation (I_p) against temperature (T_p) for the morning session for the experimental set-up recorded on April 13, 2012……56

Fig. 4.37: Linear regression analysis of solar radiation (I_w) against temperature (T_w) for the morning session for the wireless weather station recorded on April 13, 2012……..57

Fig. 4.38: Linear regression analysis of solar radiation (I_p) against temperature (T_p) for the evening session for the experimental set-up recorded on April 13, 2012……..57

Fig. 4.39: Linear regression analysis of solar radiation (I_w) against temperature (T_w) for the evening session for the wireless weather station recorded on April 13, 2012……...58

Fig. 4.40: Linear regression analysis of solar radiation (I_p) against temperature (T_p) for the morning session for the experimental set-up recorded on April 16, 2012……58

Fig. 4.41: Linear regression analysis of solar radiation (I_w) against temperature (T_w) for the morning session for the wireless weather station recorded on April 16, 2012……..59

Fig. 4.42: Linear regression analysis of solar radiation (I_p) against temperature (T_p) for the evening session for the experimental set-up recorded on April 16, 2012……..59

Fig. 4.43: Linear regression analysis of solar radiation (I_w) against temperature (T_w) for the evening session for the wireless weather station recorded on April 16, 2012……...60

Fig. 4.44: Linear regression analysis of solar radiation (I_p) against temperature (T_p) for the morning session for the experimental set-up recorded on April 17, 2012……60

Fig. 4.45: Linear regression analysis of solar radiation (I_p) against temperature (T_p) for the evening session for the experimental set-up recorded on April 17, 2012……..61

Fig. 4.46: Linear regression analysis of solar radiation (I_w) against temperature (T_w) for the evening session for the wireless weather station recorded on April 17, 2012……...61

Fig. 4.47: Linear regression analysis of solar radiation (I_p) against temperature (T_p) for the morning session for the experimental set-up recorded on April 19, 2012……62

Fig. 4.48: Linear regression analysis of solar radiation (I_p) against temperature (T_p) for the evening session for the experimental set-up recorded on April 19, 2012……..62

Fig. 4.49: Linear regression analysis of solar radiation (I_w) against temperature (T_w) for the evening session for the wireless weather station recorded on April 19, 2012……...63

Fig. 4.50: Linear regression analysis of solar radiation (I_p) against temperature (T_w) for the morning session for the experimental set-up recorded on April 29, 2012……63

Fig. 4.51: Linear regression analysis of solar radiation (I_w) against temperature (T_w) for the morning session for the wireless weather station recorded on April 20, 2012……..64

Fig. 4.52: Linear regression analysis of solar radiation (I_w) against temperature (T_w) for the evening session for the experimental set-up recorded on April 20, 2012……..64

Fig. 4.53: Linear regression analysis of solar radiation (I_w) against temperature (T_w) for the evening session for the wireless weather station recorded on April 20, 2012……...65

Fig. 4.54: Linear regression analysis of solar radiation (I_p) against temperature (T_p) for the morning session for the experimental set-up recorded on April 23, 2012……65

Fig. 4.55: Linear regression analysis of solar radiation (I_w) against temperature (T_w) for the morning session for the wireless weather station recorded on April 23, 2012……..66

Fig. 4.56: Linear regression analysis of solar radiation (I_p) against temperature (T_p) for the evening session for the experimental set-up recorded on April 23, 2012……..66

Fig. 4.57: Linear regression analysis of solar radiation (I_w) against temperature (T_w) for the evening session for the wireless weather station recorded on April 23, 2012……...67

Fig. 4.58: Linear regression analysis of solar radiation (I_w) against temperature (T_w) for the morning session for the experimental set-up recorded on April 24, 2012……67

Fig. 4.59: Linear regression analysis of solar radiation (I_w) against temperature (T_w) for the morning session for the wireless weather station recorded on April 24, 2012……..68

Fig. 4.60: Linear regression analysis of solar radiation (I_p) against temperature (T_p) for the evening session for the experimental set-up recorded on April 24, 2012……..68

Fig. 4.61: Linear regression analysis of solar radiation (I_p) against temperature (T_p) for the evening session for the wireless weather station recorded on April 24, 2012……...69

Fig. 4.62: A graph showing the mean solar radiation (I_m) against mean temperature (T_m)…….71

Fig. 4.63: Linear regression analysis of mean solar radiation (I_m) against temperature (T_m) for the morning session obtained for the entire period……71

Fig. 4.64: Linear regression analysis of mean solar radiation (I_m) against temperature (T_m) for the evening session obtained for the entire period……72

LIST OF TABLE

Table 1.1. Major Gases and trace gases found in the atmosphere……...3

CHAPTER ONE

1.0 Introduction

The energy reaching the Earth's surface in the form of direct or scattered radiation determines the temperature of both the surface of the earth and the lower atmosphere of the earth which in turn, determines the evaporation capacity and climatic features (Baro'ti *et al*, 1993).

Solar radiation (Wm^{-2}) or luminance (cdm^{-2}) refers to the short wave radiation emanating from the sun. This energy affects the Earth's weather processes as well as all environmental conditions. This radiation consists of electromagnetic radiation emitted by the sun in spectral regions (Zolta'n *et al*, 2000). A detailed diagram of the electromagnetic spectrum showing the various regions and energies associated with them on the logarithm scale is shown below.

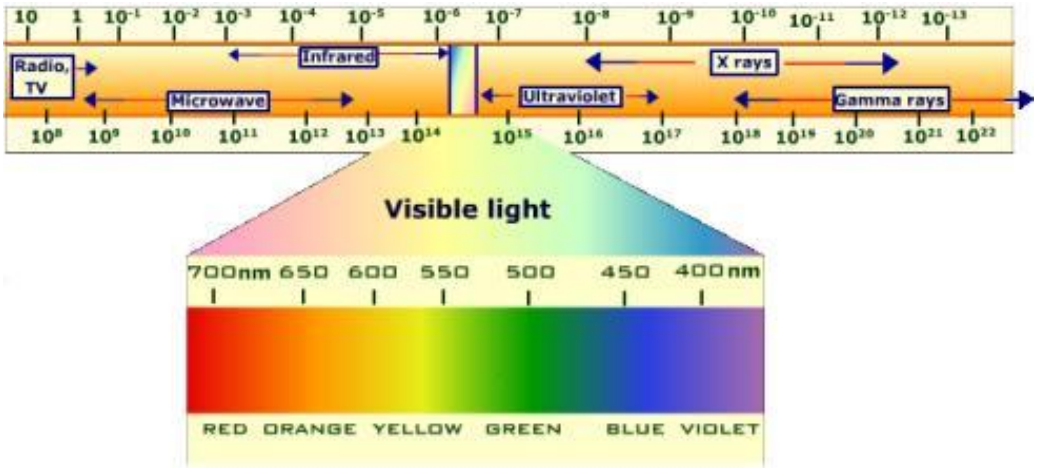

Fig. 1.1: Detailed diagram of the electromagnetic spectrum. Adapted from Wikipedia, 2012.

This spectrum covers visible light and near-visible radiation such as x-rays, ultraviolet radiation, infrared radiation, and radio waves. Both the visible and heat energy part of the sun makes life possible, and is termed as "sunshine" or "daylight". This radiation is a fundamental input for many

aspects of climatology, hydrology, biology and architecture. In addition, it is an important parameter in solar energy applications in electricity generation and in day lighting (Monteith *et al*, 1992).

The surface climate of the Earth varies, ranging from the heat of the tropics to the cold of the Polar Regions, and from draught of a desert to the moisture of a rain forest. The climate of the Earth is defined in terms of measurable weather elements. The weather elements of most interest are temperature and precipitation. Other climatic factors are very important; the humidity, the amount of water vapor in the air is related closely to the temperature and precipitation. Cloudiness influences the amount of solar radiation that reaches the surface and the trans-mission of terrestrial radiation through the atmosphere. (Liou, 2002)

Climate is therefore the synthesis of the weather in a particular region. The synthesis is therefore the combination of constituent elements or entities into a single unified entity. These elements includes; temperature, precipitation, wind, pressure, cloudiness and humidity. Soil type and distribution of vegetation is determined primarily by the local climate. The climate of a region depends on latitude, altitude, and orientation in relation to water bodies, mountains, and the prevailing wind direction (Muneer, 2004).

1.1 Composition of the atmosphere

The atmosphere is a thin gaseous envelope around the earth which comprises many gases (Murry, 1995). The majority of these gases are: Nitrogen (N_2), Oxygen (O_2), Argon (A) and Carbon dioxide (CO_2). There are other gases that exist as trace gases and these are; water vapor (H_2O), methane (CH_4), nitrous oxide (N_2O), and ozone (O_3). These gases play an important role in the energy

processes associated with life forms and are either formed or replaced by these life forms. The percentages of some of the gases found in the atmosphere are presented in the table below:

Table 1.1. Major gases and trace gases found in the atmosphere.

Gas	Percentage(%) found in air
Nitrogen(N_2)	78.084
Oxygen(O_2)	20.946
Argon(A)	0.9340
Carbon dioxide(CO_2)	0.0397
Neon(Ne)	0.001818
Methane(CH_4)	0.000179
Ozone(O_3)	0.0000009

Nitrogen is removed from the atmosphere and deposited at the Earth's surface mainly by nitrogen fixing bacteria and by way of lighting through precipitation. Oxygen, which is one of the main gases in the atmosphere primarily, exists by its exchange between the environment and life forms through Photosynthesis and respiration processes.

The next abundant gas is water vapor whose concentration in the atmosphere varies both spatially and temporally depending on a particular location and region. The functions of the water vapour gas includes but not limited to:

1. Redistribution of the heat energy of the Earth through latent heat energy exchange.
2. Warming the Earth's surface through green-house effect, and
3. Condensation processes that later precipitates and falls as rain.

The next abundant gas is carbon dioxide (CO_2). The volume of this gas which is an important greenhouse gas has increased over the past years. The increase is as a result of deforestation, burning of fossil fuels, etc. This gas is normally exchanged between the atmosphere and life forms through the processes of photosynthesis and respiration.

To have a better understanding of the interactions between the solar radiation energy and the biosphere, a critical look at the composition of the atmosphere must be taken into consideration.

1.2 Atmospheric structure and temperature

Temperature is the most widely recognized climatic variable. The global average temperature at the surface of Earth is 15°C. The extremes of recorded surface temperature range from the coldest temperature of -89°C at Vostok, Antarctica, to the warmest temperature of 58°C at Alziziyah, Libya. These temperature extremes reflect the well-known decrease of temperature from the tropics, where the warmest temperatures occurs, to the Polar Regions, which are much colder (Badescu, 2008).

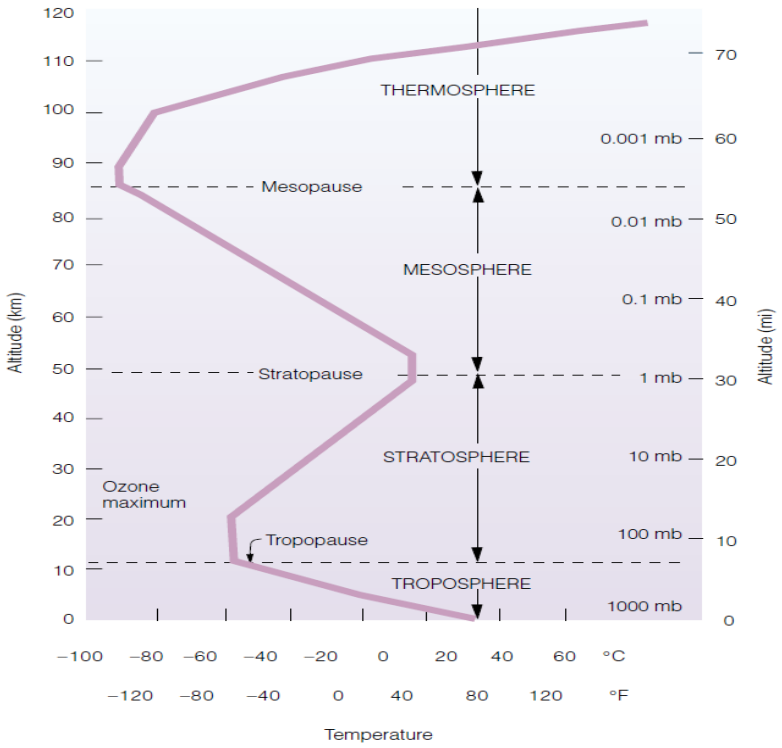

Fig 1.2: Layers of the atmosphere as related to the average profile of air temperature above the Earth's surface. The heavy line illustrates how the average temperature varies in each layer. Adapted from Ahrens, 2006.

An important feature of the temperature distribution is the decline of temperature with height above the surface in the lowest 10-15km of the atmosphere. This rate of decline, called the Lapse rate is defined by

$$\Gamma = -\frac{dT}{dz} \tag{1.1}$$

Where T is the temperature in K and z is the altitude in meters (m). The Global mean tropospheric lapse rate is about 6.5Kkm^{-1}, but the lapse rate varies with altitude, season, and latitude. In the upper stratosphere, the temperature increases with height up to 50km. The increase of temperature with height that characterizes the stratosphere is caused by the absorption of solar radiation by

ozone. Above the stratopause at about 50km the temperature begins to decrease with height in the mesosphere. The temperature of the atmosphere increases rapidly above about 100km because of the heating produced by absorption of ultraviolet radiation from the sun which dissolves oxygen and nitrogen molecules and ionizes atmospheric gases in the thermosphere. The decrease of temperature with altitude in the troposphere is crucial to many of the mechanisms whereby the warmth of the surface temperature of Earth is well-known. The lapse rate and temperature in the troposphere are determined primarily by a balance between radiative cooling and convection of heat from the surface.

A region of negative lapse rate is called a temperature inversion. It arises because the surface cools very efficiently through emission of infrared radiation in the absence of insolation. The air does not emit radiation as efficiently as the surface and heat transported pole ward in the atmosphere keeps the air in the lower atmosphere warmer than the surface.

The Physics Department of the Legon campus of the University of Ghana, which is situated in the Accra metropolis, enjoys tropical savannah climate with a little variation in temperature throughout the year. With an elevation of 97 meters, the monthly mean temperature of the place ranges from 24.3°C, which is the coolest in August, to 27.5°C in April. The site has a sunrise at 6:00 hr local time and a sunset of 18:00 hr local time during the period of observation.

1.3 The climatic regions of Ghana

The climate in most of Ghana is wet and dry tropical which is strongly affected by the West African Monsoon. The movement of the Inter-tropical Conversion Zone (ITCZ) which oscillates between the Northern and Southern tropics over the course of the year is responsible for the rainfall patterns of Ghana (McSweeny *et al*, 2010). The Inter-tropical Convergence Zone is a region of light winds which occur on or at the Equator. At this region, because there is average solar radiation, the air is warmed at the surface which causes it to rise. This rising of the air creates a band of low pressure which is therefore replaced by the trade winds by approaching the equator from both the north and south directions. The convergence of these trade winds creates a zone of cumulus clouds and attendant shower activity. The position of the Inter-tropical Convergence Zone drastically affects rainfall patterns resulting in the wet and dry seasons of the country. Wet and dry tropical climates are marked by warm to hot temperatures throughout the year, and abundant rainfall in only one season. This condition is noticeable in Northern Ghana where there is a single wet season from May to November when the ITCZ is in its northern position and the prevailing wind is south-westerly, because of less annual rainfall and the strictly seasonal nature of the rain. The northern and central parts of Ghana receive 150-250mm of rainfall per month in the peak months of the wet season (July to September). A second climate region exists in southwestern Ghana. The southern regions of Ghana have two wet seasons, one from March to July and a relatively shorter one from September to November, corresponding to the north and south passages of the ITCZ across the region. Ghana has warm to hot temperatures throughout the year because of its proximity to the Equator and its relatively low elevation. The average annual temperature in Accra, Ghana is 24-32°C in the warmest season which occurs in January, February, and March. The northern section of Ghana has hotter temperatures of 37-41°C in April, May, and June and lowest in July, August

to September with temperatures of 36-43°C because the ITCZ is farthest from the moderating influence of the ocean, and closest to the Sahara (GMA, 2011). In this respect, it is estimated that the monthly average solar irradiation is between 4.4 and 5.6 KWh/m^2/day and the sunshine duration is between 1800 and 3000 hours per annum (Appiah and Donkor, 2011). With these values of solar radiation and temperature, it is therefore important to study the relationship between temperature and the solar radiation of a particular location.

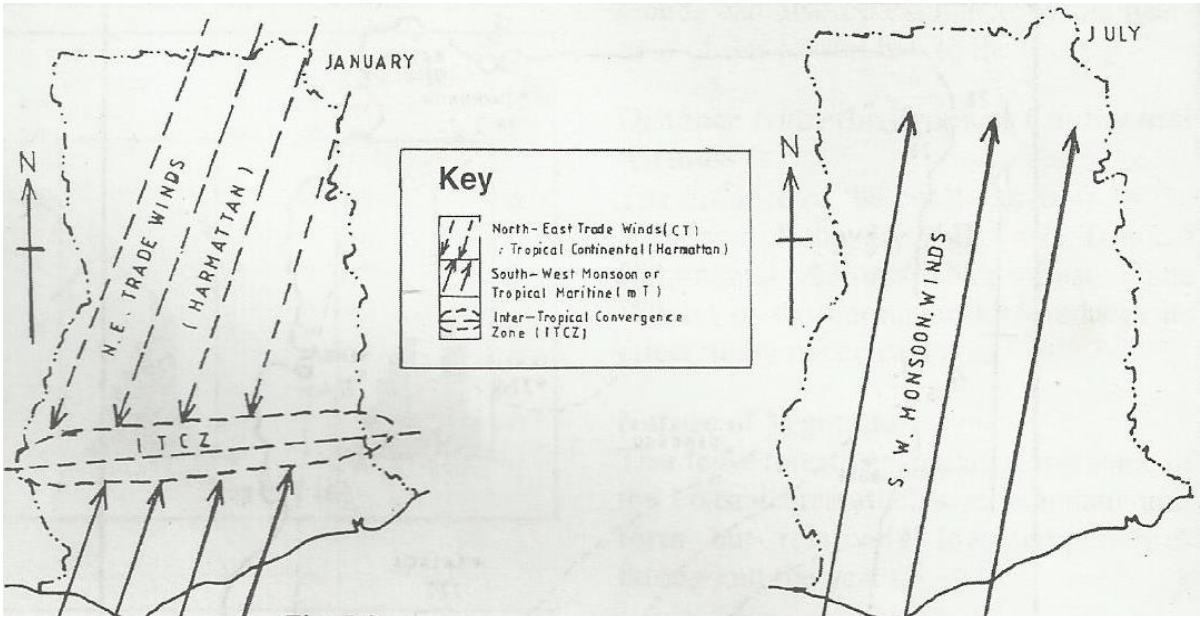

Fig 1.3: Map showing the intercontinental convergence zone describing the prevailing winds necessary for the two main seasons in the country (Adapted from Ghana Meteorological Agency, 2002)

1.4 Solar radiative transfer

The source of the energy that sustain life on Earth is the sun. The basic global energy balance of the Earth is between energy coming from the sun and the energy returned to space by Earth's radiative emission. The absorption of solar radiation takes place mostly at the surface of Earth, whereas most of the emission to space originates in its atmosphere.

The energy reaching the Earth's surface in the form of direct or scattered radiation determines the temperature of both the surface and the lower atmosphere, which in turn determines the evaporation capacity and climatic features.

The radiation reaching the Earth has different values during the year. This fluctuation results from the Earth's movement in an elliptic orbit and from the obliquity (in relation to the elliptic orbit) of the rotation. (Sza'cz *et al*, 1997).

The first law of thermodynamics states that energy is conserved. The first law for a closed system may be stated as, "The heat added to a system is equal to the change in internal energy minus the work extracted." This law may be expressed mathematically as

$$dQ = dU - dW \tag{1.2}$$

Where dQ, the amount of heat added, dU is the change in internal energy of the system, and dW is the work extracted from the system. Heat can be transported to and from a system by the processes of Radiation, Convection and Conduction. The transmission of energy from the sun to Earth is almost radiative.

The figure below shows the modification of solar radiation by atmospheric and surface processes for the whole Earth over a period of one year. Of all the sunlight that passes through the atmosphere annually, only 51% is available at the Earth's surface to do work. This energy is used to heat the

Earth's surface and the lower atmosphere, evaporate water, and run photosynthesis in plants. Of the other 49%, 4 is reflected back to space by the Earth's surface, 26% is scattered or reflected to space by clouds and atmosphere particles, and 19% is absorbed by atmosphere gases, particles and clouds.

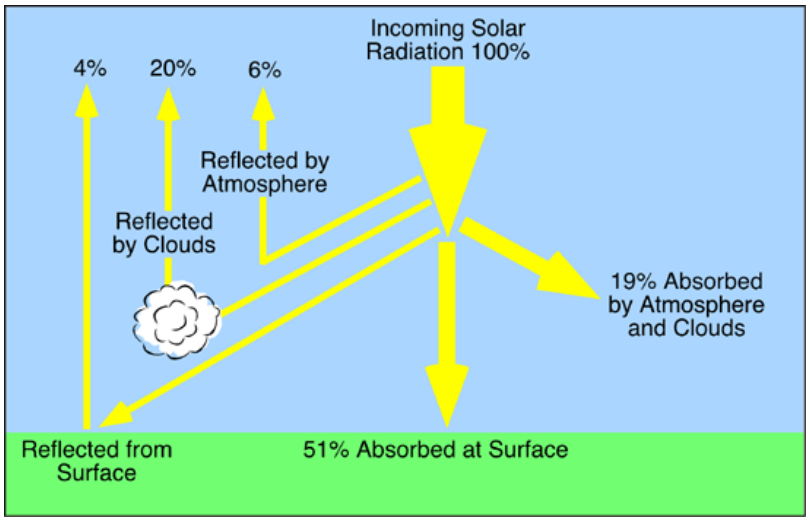

Fig 1.4: Interactions associated with the absorption and distribution of solar radiation on the Biosphere. Adapted from Fundamentals of Physical Geography.

1.5 Measurement of solar radiation

The solar radiation that passes through the atmosphere is partially absorbed by the constituents of the atmosphere, partially reflected back to space, and is partially diffused with the remaining reaching the ground as direct solar radiation.

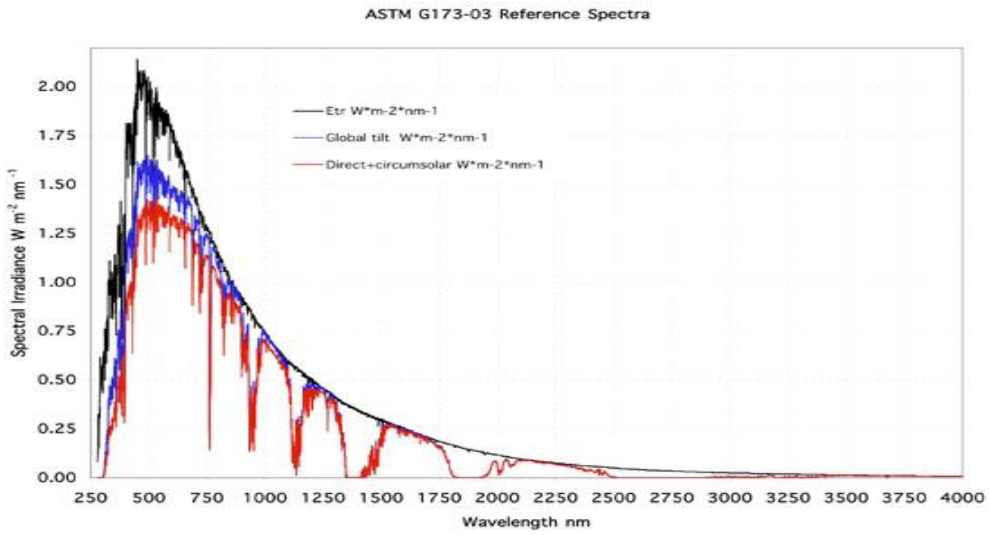

Fig.1.5: Extraterrestrial solar spectrum. Adapted from Geymard, 2004.

Diffuse solar radiation is that solar radiation received from the sun after its direction has been changed by reflection and scattering by the atmosphere. It has no fixed direction at any instant. It is scattered in all directions (Salam *et al*, 1978).

Solar radiation consists of electromagnetic radiation emitted by the sun in spectral regions ranging from X-rays to radio waves. The "optical radiation" spectrum with a spectral range of about 300-4000nm in the terrestrial region has applications in renewable energy which utilizes this particular radiation. The determination of this radiation has changed over time with respect to measurements from terrestrial observatories and space borne instruments, modeled calculations or a combination of these. (Gueymard, 2004)

The spectral integration of the Extraterrestrial solar spectrum over all possible wavelengths (0 to infinity) is usually referred to as the "Solar constant" or "Air mass zero" (AM0) spectrum. Since

the sun's output is not constant but varies slightly over short (daily) to long periods, the name Total Solar Irradiance has been introduced. (Fröhlich *et al*, 1998)

Terrestrial solar radiation measurements are based on Pyranometers that respond to radiation with a hemispherical field view, or Pyrheliometers, narrow field view of instruments (5.8° to 5.0°) that measure the nearly collimated (i.e. parallel rays) radiation from the 0.5° diameter solar disk and a small part of the sky.

The total hemispherical radiation (Global radiation), G, on a horizontal surface is the sum of the direct beam, B, projected on the surface (modified by the cosine of the incidence angle of the beam), I, and the sky radiation (diffuse beam), D. The direct solar radiation is observed from sunrise to sunset, while global solar radiation is observed in the twilight before sunrise and after sunset, despite its diminished intensity at these times. The expression for these radiations is given as:

$$G = Bcos(I) + D \tag{1.3}$$

Where I is the angle between the solar disk and the normal to the horizontal surface.

The direct beam or direct normal solar radiation is measured by a Pyrheliometer on a sun-following tracker. The diffuse solar radiation is measured by a shaded pyranometer under a tracking ball, and the global horizontal solar radiation component is measured by a pyranometer with a horizontal sensor.

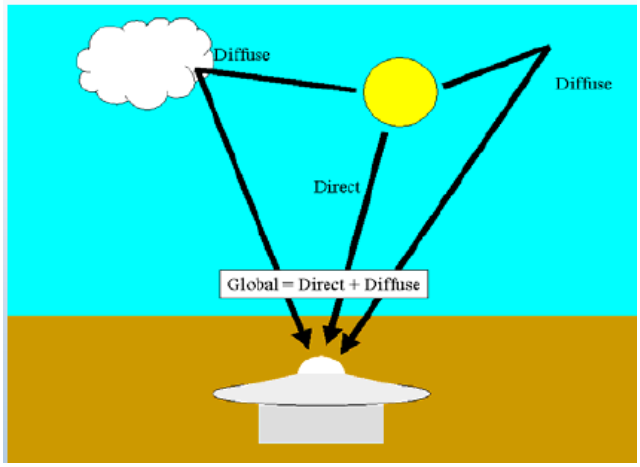

Fig1.6: Distribution of the solar radiation components. Adapted from Stoffel and Wilcox, 2004

1.6 Instruments used in measuring solar radiation

There are various instruments used to measure the amount of solar radiation falling on the Earth's surface. These includes; Pyranometers, Reference cells, and Pyrheliometers.

Pyranometers respond to the change in temperature when the sunlight heats a black surface. The pyranometer gives a voltage signal that is directly proportional to the irradiance as measured in watts per square meter. The pyranometer is specially designed to accept light from all angles. The pyranometer have a flat response to light from the ultraviolet to the far infrared, and also have a stable output regardless of sky conditions and changing ambient conditions. These instruments are calibrated once a year since their output can drift.

Fig 1.7: Pyranometer for measuring global horizontal radiation. (Adapted from Stoffel and Wilcox, 2004)

Reference cells on the other hand measures solar irradiance by using photons with energy above the band gap of a PV material. This energy is then converted directly into positive and negative charges that can be collected and used in an external circuit. The reference cell generates a current that is dependent on the number and spectral distribution of the photons. Typically, the current of the reference cell is measured by measuring the voltage across a small resistor that is included in the reference cell package. The cell's voltage calibration is under the reference spectrum [ASTM G173, or IEC 60904-3 spectrum] at 1000 Wm^{-2}, 25°C using the standard techniques [IEC 60904-1] (Emery and Kurtz, 2012).

The reference cell does not respond to photons of energy less than the band gap, implying that they will be insensitive to changes in this part of the spectrum when used to quantify the broadband meteorological irradiance. The attributes that introduces the uncertainty when reference cells are used to characterize the weather are the same as the attributes that make them more ideal for characterizing the PV system performance.

The next instrument is the Pyrheliometer. This instrument is used for measuring the direct part of the solar irradiance (Kipp and Zonen, 2004). Sunlight (the wavelengths of electromagnetic radiation that the sun gives) enters the window and is directed onto a thermopile which converts heat to an electrical signal that can be recorded. (Stoffel and Wilcox, 2004)

1.7 Objectives of this work

- To use a second class pyranometer to detect and measure incoming solar radiation intensity and hygro-thermometer to measure temperature within the study area.
- To correlate recorded temperature and corresponding solar radiation of different days.
- To verify obtained equations with data from an automatic wireless weather station.

1.8 The study area

The Physics department of the University of Ghana is located about 20 km from the coastal shores of Accra and also about 13 km from the city center. It is an area that receives most sunshine with a wet season covering between the months of April through to July.

The campus has an average humidity of about 58 % around 1400 hr local time and around 86 % during 1900 hr local time. An average of annual rainfall figure of about 215 mm is recorded in and around the campus (GMA, 2011).

1.9 Motivation for the study

There's a growing need to assess the potential of the various renewable energy sources of the Earth. Geothermal, Hydro, Wind and Solar Energy are some of the examples of the renewable sources of energy which can be harnessed to supplement the other non-renewable sources of

energy. The sun which is the driving force of all energy processes and all atmospheric process radiates solar energy, and this form of energy can be trapped and used in various ways. Its usage produces less carbon dioxide emissions into the atmosphere thereby not contributing to the excessive pollution being done by other sources such as fossil fuels. There's therefore the growing need to study this type of energy in order to come out with relevant solutions and practices to harness this type of energy. The purpose of this research work is related to and includes the following:

- To show that with the use of simple apparatus, empirical relationships between solar radiation and temperature can be obtained without the use of sophisticated equipment.
- To gain knowledge about the instant solar radiation obtained at a particular location and place.
- To be able to predict the values of temperature and instant solar radiation when equipment are not readily available from the obtained relations.

1.10 Literature review

Due to the availability of solar radiation at the Earth's surface, it is therefore essential to determine its use in applications such as in solar thermal systems which including solar hot water heater and passive systems, Agriculture (evapotranspiration), and in many fields such as telecommunication and industrial applications. There are several models which can determine the amount of solar radiation at a particular location based on certain environmental parameters such as maximum and minimum temperature, clear sky index, relative humidity, wind direction and speed, and amount of cloud cover. These models have been developed to estimate the irradiance at different places in

the world. But because of the differences in local climatic conditions, the suggested radiation models for one location may not successfully apply to other places.

Kimball (1919) was the first to propose a linear correlation between actual sunshine duration, actual global irradiation, and a global irradiation for a cloudless sky. Global solar radiation estimation from sunshine duration was mathematically initiated by Angström (Angström, 1924). Several researchers have used different methods or models to estimate the solar energy based on a single environmental parameter or a combination of parameters (Gueymard, 2003). Some of these researched models include atmospheric transmittance model (Campbell *et al*, 1998), clearness index model (Reindl *et al*, 1990) and diffuse fraction model (Batlles *et al*, 2000).

Dimas, Syed, and Shiraz (2011) conducted research into the estimation of hourly solar radiation using ambient temperature and relative humidity data over the Ipoh city area (Dimas *et al*, June 2011). Solar radiation data are not always available for a particular location, even if there's a weather station near the area, the data may contain missing data. This might be due to sensor error or damage. An estimation method is therefore required to fill the missing data. In this study, missing data of solar radiation was estimated using two different methods, first, beam atmospheric transmission determination with measured relative humidity and ambient temperature data and the second method using relative humidity-beam transmittance correlation. This study therefore proposed clearness-index beam transmittance numerical correlation method using measured data in Universiti Teknologi PETRONAS, Bandar Seri Iskandar.

Out of all the environmental parameters, the parameters that were measured for this study were; solar radiation, ambient temperature, relative humidity, speed and direction of wind. The data on ambient temperature and relative humidity were used to estimate the solar radiation.

Based on the two methods used, it was therefore found that method I performed better than method II with minimum correlation coefficient of 0.95, RSME of 87.6 Watt/m^2, NSRME of 8.29%, and index of agreement of 0.97. These prediction methods were intended to fill the missing data in the measured data of solar radiation to get the complete time series data.

Bajpai and Kalpana (2009) studied the estimation of instant solar radiation by the use of instant temperature. Their study required the use of a Solarimeter to measure the solar radiation and a digital thermometer to measure the temperature over Lucknow, India. The main objective of this work was primarily to use a simple regression analysis to estimate instant solar radiation using instant temperature. A complete data set for a day was used starting from 7:30 am to 6:00 pm. Their results obtained from this study indicated that the equations derived with their accompanying percentage errors, instant solar radiation can therefore be estimated using instant temperature data values. The process through which they obtained the equations are based on the exponential relation as

$$y = AB^x \tag{1.4}$$

The software tool EXCEL to obtain the relation below;

$$y = 3E - 26e^{0.2117x} \tag{1.5}$$

With the manual calculation, they had the relation by applying the principle of logarithms to (1.4) and the obtained the equation below;

$$R = 2.88204(10^{-26})e^{0.211622755T} \tag{1.6}$$

With the measured and calculated values of radiation, they found a percentage error in the value of the solar radiation and plotted a graph of both calculated values of solar radiation and measured

from equation with temperature and found out that, they fitted perfectly. This process was also carried out for the evening session as well.

Adukpo and Akpan (2009) researched into the estimation of horizontal solar radiation in three geographical regions of Ghana using sunshine duration. Their study conducted used three practical models which are Iqbal's (1979), Gariepy's (1980), and Rietveld's (1978) models to estimate the horizontal global solar radiation. The data for this particular research was taken from the Ghana Meteorological Agency. These models were employed with the aim of establishing the most prudent one in prediction of solar radiation in six different locations in Ghana where no solar radiation in the form of beam or diffuse was available. Adukpo and Akpan selected these locations on transect basis to represent the different climatic zones of Ghana which are the coastal grassland, the tropical rain forest and the guinea savannah.

The models for this particular study were selected because the parameters that were used were easily available for the locations of this particular study. With these chosen models and the selected parameters, it was noted that the amount of horizontal global solar radiation obtained in Ghana was found to be in the range between 11.37 MJ/m^2/day and 22.09 MJ/m^2/day when using them. It was also observed that, Iqbal's model gave a better estimation in the coastal zones while Gariepy's model gave better estimation in the middle and northern regions of the country.

Bristow and Campbell researched into the relationship between incoming solar radiation and daily maximum and minimum air temperature (Bristow and Campbell, 1984). The relevant data for this particular study was collected on a daily basis at Pullman on a latitude of 46° 46' N, longitude 117° 12' W and an elevation of 776 m between 1 June 1980 and 31 May 1981. The temperature extreme data values were recorded at screen height while daily irradiance was recorded with an Eppley pyranometer. The main objective of this research was to show that a suitable relationship exists

between solar irradiance and the range in daily temperature extremes. The daily temperature extremes were calculated using the relation,

$$\Delta T(J) = T_{max}(J) - T_{min}(J) \tag{1.7}$$

Where T_{max} is the maximum temperature and T_{min} is the minimum temperature. ΔT is the change in temperature between the daily maximum and minimum temperatures and J is the day number.

The daily total transmission coefficient (T_t) was used instead of using the measured daily solar irradiance in relating radiation and ΔT. The total transmission coefficient T_t incorporates atmospheric attenuation coefficients. Its relation was found to be,

$$T_t = \frac{daily\ measured\ irradiance}{daily\ extraterrestrial\ insolation} \tag{1.8}$$

Computed and measured irradiance data were then compared in an attempt to validate the technique. The equation that was used to describe T_t as a function of ΔT was found to be

$$T_t = A[1 - \exp\{-B(\Delta T)^C\}] \tag{1.9}$$

Where A, B and C are empirical coefficients. A represents the maximum clear sky, T_t characteristics of the study area where B and C determine how soon maximum T_t is achieved as ΔT increases.

CHAPTER TWO

THEORY

2.0 Nature of Electromagnetic radiation

Electromagnetic radiation is a form of energy derived from oscillating magnetic and electrostatic fields. It is one of the forms of energy that is capable of transmission through empty space with a velocity of $c = 3.0 \times 10^8 ms^{-1}$. The frequency ϑ of oscillation is related to the wavelength $\lambda$by the relation;

$$c = \nu\lambda \tag{2.1}$$

and the wave number

$$k = \frac{2\pi}{\lambda} \tag{2.2}$$

Is sometimes used as an index of frequency.

Solids, liquids and gases absorb and emit radiation based on the changes in the energy state of the atoms and molecules. The principle of energy conservation is fundamental to the material origin of radiation. The amount of radiant energy emitted by an individual atom or molecule is equal to the decrease in the potential energy of its constituents.

2.1 Blackbody radiation and the radiation laws

Kirchhoff (1895) examined the relationship between radiation absorbed and emitted by matter. He defined two separate terms in this relationship as absorptivity and emissivity. The absorptivity of a surface $\alpha(\lambda)$ is the fraction of incident radiation absorbed at a specific wavelength λ and the

emissivity $\varepsilon(\lambda)$ as the ratio of the actual radiation emitted at a wavelength (λ) to a hypothetical amount of radiant flux **B (λ).** He considered that the thermal equilibrium of an object inside an enclosure at a uniform temperature, the absorptivity, $\alpha(\lambda)$ is always equal to the emissivity, $\varepsilon(\lambda)$. In the case of an object where the emissivity $\varepsilon(\lambda)$=1 at all wavelengths, the spectrum of the emitted radiation is known as a black body spectrum. Kirchhoff's radiation law is represented mathematically as;

$$\alpha(\lambda) = \varepsilon(\lambda) \tag{2.3}$$

Kirchhoff law (2.2) indicates that, at the same wavelength, good emitters are equally good absorbers.

The basic law of radiant emission of energy is the Planck's law (1900) which is given as

$$E_\lambda * = c_1/[\lambda^5(\exp(\frac{c_1}{\lambda T}) - 1) \tag{2.4}$$

Where $E_\lambda *$= amount of energy $Wm^{-2}\mu m^{-1}$ emitted at wavelength $\lambda(\mu m)$ at temperature T (K)

$c_1 and\ c_2$=$3.0 \times 10^8 ms^{-1}$ and $\lambda(\mu m) = 1.44 \times 10^4 \mu m$.

This law is clearly stated as "A fundamental law of quantum theory where the energy associated with electromagnetic radiation is emitted or absorbed in discrete amounts which are proportional to the frequency of radiation.

Wien's (1896) deduced that the maximum energy per unit wavelength should be emitted at a wavelength λ_m given by;

$$\lambda_m = \frac{2897}{T}\ \mu m \tag{2.5}$$

Where T= temperature and λ = wavelength.

This law takes into consideration measurements using a combination of a spectrometer and a sensitive thermopile thereby establishing that the spectral distribution of radiation from a full radiator is a curve in which the chosen temperatures of 6000K and 300K correspond approximately to the black body temperatures of the sun and the earth's surface (Henderson and Robinson, 1994).

Stefan-Boltzmann also formulated a law that related the Energy flux density being proportional to the fourth power of its absolute temperature. Because the energy flux density is proportional to the fourth power of its temperature, emission of radiation from earthly bodies changes considerably, even in the limited temperature range characteristic of a single day or a short season. The law can be mathematically stated as;

$$E = \sigma T^4 \qquad (2.6)$$

Where E= energy flux density, σ = Boltzmann's constant which is $5.67 \times 10^{-8} Wm^{-2}K^{-1}$ and T is the temperature measured in kelvin.

From the stated laws and principles, it is clear that the flux density and wavelength of maximum emission are functions of the temperature of the radiating body.

2.2 The cosine law of emission and absorption

The temperature which determines the total flux of energy emitted by a surface can be estimated by measuring the radiance of the surface with an appropriate equipment.

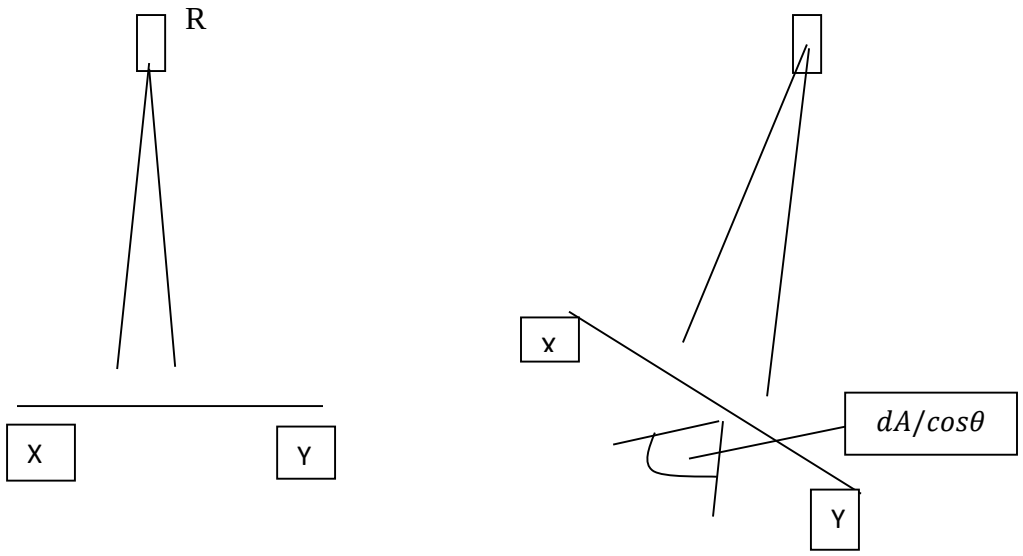

Fig. 2.1: The amount of radiation intercepted by a radiometer from the surface XY is independent of the angle of emission, but the flux emitted per unit area is proportional to $cos\theta$. Adapted from Monteith, 1973.

As the source of a full radiator will appear to have the same temperature whatever angle it is viewed from, the intensity of radiation emitted from a point source on the surface and the radiation of an element of surface must both be independent of θ. On the other hand, the flux per unit solid angle divided by the true area of the surface must be proportional to $cos\theta$ as shown in the figure above.

A radiometer R mounted vertically above an extended horizontal surface XY sees an area, dA. When the surface is tilted through an angle, θ, the radiometer now sees a larger surface $dA/cos\theta$, but provided the temperature of the surface stays the same, its radiance will be constant and the flux recorded by the radiometer will also be constant. It therefore follows that the flux emitted per unit area (the emitance of the surface) at an angle θ must be proportional to $cos\theta$ so that the product of emitance and the area emitting to the instrument stays the same for all values of θ.

2.3 The Pyranometer and its theory of operation

Solar radiation measurements can be carried out with the appropriate equipment depending on what is observed at the particular location. For the purpose of this research, a Pyranometer is used. Detailed structure of the Pyranometer is shown in the figure below.

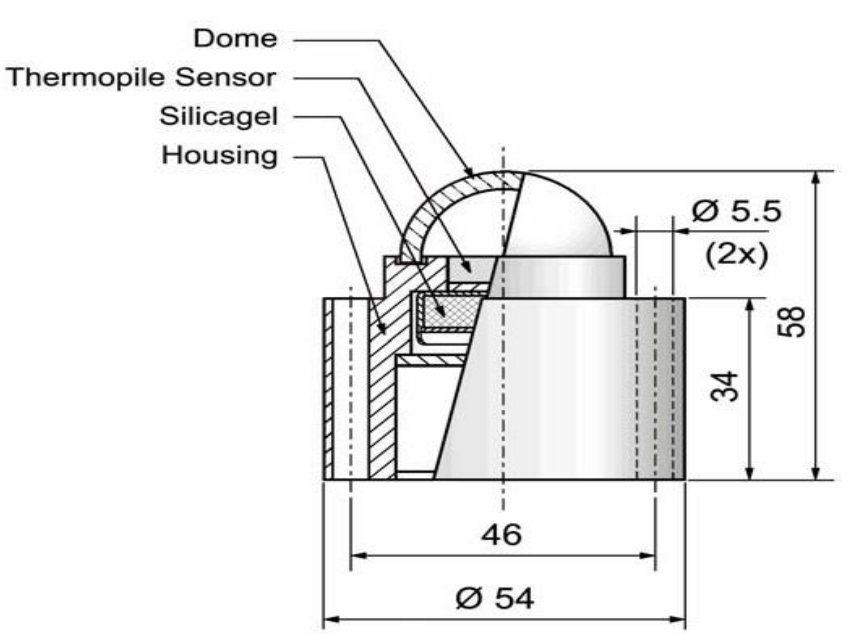

Fig. 2.2: Construction details of a Pyranometer (Adapted from Kipp and Zonen instruction manual, 2004)

The Pyranometer (thermo-pile type) is the standard tool for measuring solar radiation in Meteorology by integrating the solar radiation input over the whole spectrum and when mounted horizontally, over the effective part of the solid angle (Haeberkin *et al*, 1995). Pyranometer measure truly available solar irradiation. This tool consists of a thermopile sensor, a dome and a cable all enclosed in a housing. The thermopile is coated with a black absorbant coating. The paint

absorbs the radiation and converts it to heat. The resultant energy flow is converted to a current by the thermopile. Spectral specifications are determined by the thermopile and the dome.

This tool is designed in such a way that it receives homogenous (uniform) radiation over the collector surface by measuring the solar energy that is received from the whole hemisphere (180° field of view). Because of the fact that it has a flat spectral sensitivity from 0.3 to 3 microns, its calibration is valid for natural sunlight and for most types of artificial light (xenon lamps, halogen lamps) (Kipp and Zonen instruction manual, 2004).

CHAPTER THREE

METHODOLOGY

3.0 Measurement of meteorological parameters

Various equipment and techniques are being employed to read and record meteorological observations based on what parameters are been studied. The observational methods used to measure these atmospheric or meteorological parameters are grouped into two main categories which are surface-based subsystems and space-based subsystems (WMO, 1990). Some of the equipment been used for these surface-based subsystems includes; the Stevenson screen, transmissometer, thermograph, weather radar, etc. Most of the parameters being observed by certain meteorological stations include: Present weather, past weather, wind direction and speed, amount of cloud, type of cloud, height of cloud base, visibility, temperature, and relative humidity. Some of these stations that house most but not all of this instruments are the Stevenson screen and the Davis Wireless Weather Station.

The Stevenson screen is meteorological equipment that houses instruments particularly thermometers and thermo hydrographs, so that they are well ventilated but protected from direct radiation. But with the purpose of this research that deals with the relationship between incoming solar radiation and daily maximum and minimum temperature, a weather station is required. Such equipment is the Davis wireless weather station: Vintage Pro 2 Plus (fig 3.1). This weather station uses frequency hopping spread spectrum radio technology to transmit weather data wirelessly up to 1000ft (300m). Because of this frequency band, all temperature and solar radiation measurements may be obtained using this weather station.

3.1 Experimental set-up

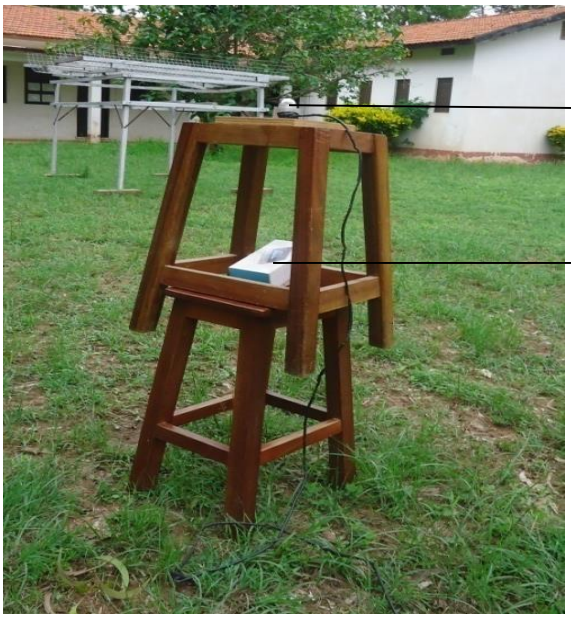

Fig. 3.1: Diagram showing the different equipment used for data collection at the Department of Physics, Legon.

Solar radiation data were obtained in the Department of Physics using Kipp and Zonen CM3 Pyranometer which has a constant of 21.3 $\mu V/Wm^{-2}$ connected in series to a PHYWE amplifier

and a voltmeter. To obtain the actual values of the solar irradiance, the pyranometer was mounted on a stand to a height of about 1.3 m. The pyranometer has a low intensity signal output so the value was amplified using a PHYWE amplifier. The amplifier has a time constant of 1 s and an amplification of 10^3. The amplification value of 10^3 slows down the readings on the voltmeter and enables the recording of the actual solar radiation values over the time period of 5 min using a stop watch.

With the constant on the pyranometer and the readings obtained from the voltmeter, the solar irradiance at that instant or particular time can be obtained using the following relation employing the idea of ratio and proportion.

$$1 W m^{-2} = 21.3 \mu V \qquad (3.1)$$

The value obtained after calculating the solar irradiance is then divided by the amplification value of 10^3 to give you the actual value of the solar irradiance. The temperature and relative humidity values were obtained using a hygro-thermometer.

3.2 Data acquisition using the automatic wireless weather station

Fig. 3.2: Davis Wireless Weather Station: Vintage Pro2 Plus (Adapted from Davis Instruments, Davis, CA, USA)

Environmental parameters may be measured by a variety of instruments depending on what parameter is needed or required. This weather station has a versatile sensor suite that combines rain collector, temperature and humidity sensors and anemometers in one package. This weather station is designed to use frequency hopping spread spectrum radio technology to transmit weather data wirelessly up to 300m (1000ft). The Davis Wireless Weather station has the following features: its electronic components are enclosed in a weather-resistant container; it has a laser-calibrated rain collector; it can track (high, low, total. Averages) for almost all the environmental variables; it has a data logger and a software attached to it. Apart from the features, this weather station is designed to have the following components that enable data to be collected accurately. It has a solar powered ISS (Integrated Sensor Suite); Console (which is both an Emitter and a Receiver); Anemometer probe (to measure the wind direction); Irradiance probe; UV probe; Data

logger; and a weather link (software to manage the data collection process). This weather station measures most of the atmospheric parameters such as: Solar radiation or UV; Temperature; Wind; Rainfall; Barometric Pressure; Relative Humidity; Heat Index or Dew point; Sunset, Sunrise; Moon Phase; and Forecasting.

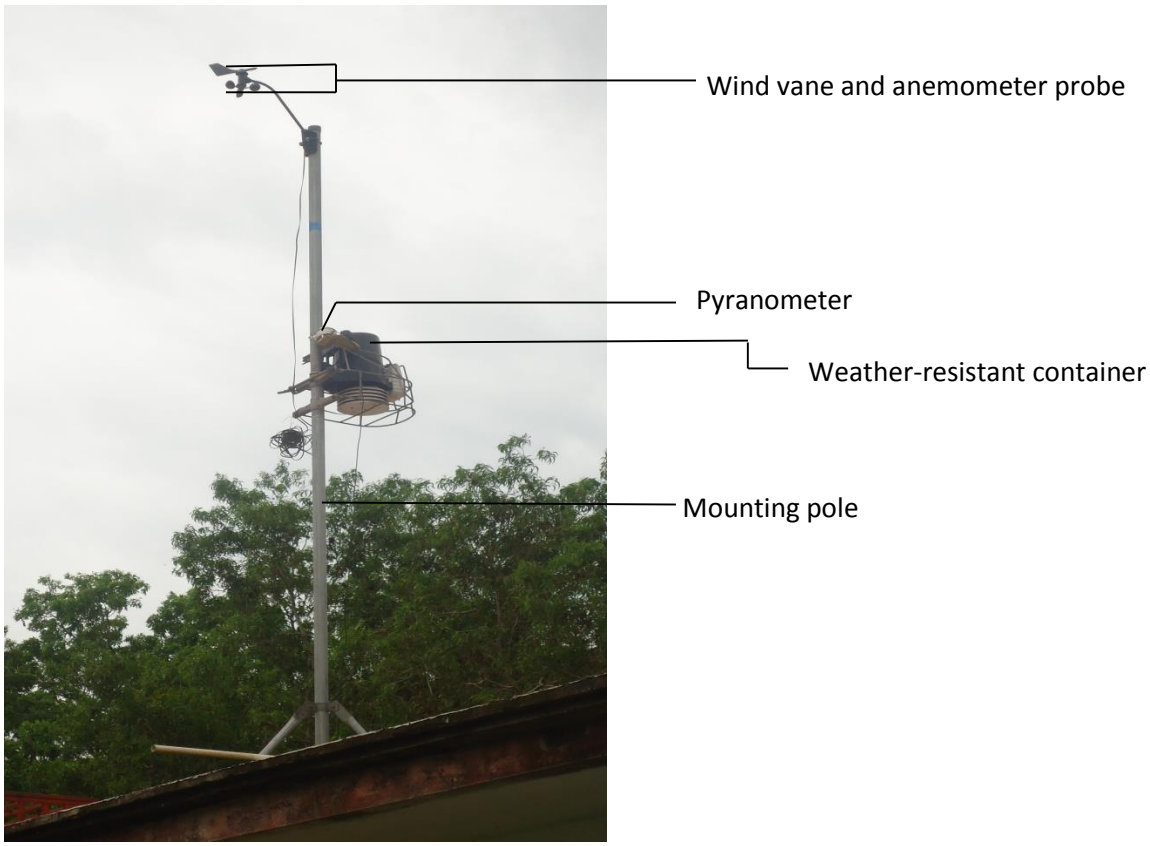

Fig. 3.3: Picture of a mounted Davis Wireless Weather Station at the Department of Physics, Legon.

The equipment is mounted at a distance of 102.4 m above sea level with the following geographical coordinates:

Latitude: 5°39’04N

Longitude: 0°11’04N

This equipment measures uses the ISS (Integrated Sensor Suite) temperature sensor to measure the outside temperature. It does this by either sampling the temperature at the end of the archive period and writes it to a data logger having a USB interface which is connected to a remote computer containing the software weather link or samples the temperature throughout the archive period and calculates an average value at the end. In this case, the archive period used for this equipment was 8s. This means that after every 8s, the equipment collects data of temperature readings and averages the values and gives the actual temperature value after the 5min period. In this case solar radiation data is also collected in the same manner as the temperature data is taken.

3.3 Data collection: measuring solar radiation, temperature and relative humidity

Three parameters were studied in this work, i.e. the daily air temperature, the amount of solar radiation, and the relative humidity. Other atmospheric parameters which were not considered were: the rainfall, the amount of cloud cover, and sunshine duration, and wind speed.

This involves recording the solar radiation measured by the dome of the pyranometer and the corresponding voltage as well as the corresponding time the voltmeter recorded the values. The air temperature during the entire duration of the recording of the solar radiation was also recorded as well as the relative humidity using the hygro-thermometer. The relative humidity was measured because it had an indirect effect on the temperature of a particular location. Relative humidity refers to the amount of water vapor contained in the air at a given temperature relative to the total amount of water vapor the air is capable of holding at that temperature. Hence, the relative humidity will decrease if the temperature increases and it will therefore increase if the temperature is lowered.

Data was collected for a period of approximately one month and the result obtained is presented in chapter four of this report.

3.4 Data collection using the experimental set-up

The Pyranometer reads data of the solar radiation at a particular location based on the zenith angle of the sun and the cosine response of the Pyranometer. A Pyranometer has a directional response which is equal to the cosine law. A perfect cosine response will show maximum sensitivity of 1 at an angle of incidence 0° (perpendicular to the sensor surface) and zero sensitivity at an angle of incidence 90° (radiation passing over the sensor surface). In between 0° and 90° the sensitivity should be proportional to the cosine of the angle of incidence (Kipp and Zonen, 2004)

As light from the sun hits the dome of the Pyranometer, a voltage is generated and it is recorded by the voltmeter. Using the constant on the Pyranometer, the solar radiation at that instant can be calculated from the voltage measurements as follows;

$$1\frac{W}{m^2} = 21.3\mu V \qquad (3.2)$$

Where $1\mu = 10^{-6}$

Hence, a voltage reading of $0.09V$at a time of 6:00 local time will have a corresponding solar irradiance value as;

$$\Rightarrow 0.09V = \frac{0.09V}{21.3 \times 10^{-6}V} \times \frac{1W}{m^2}$$

$$= 4225.3521\, W/m^2$$

This voltage value is then divided by the amplification constant of 10^3 which gives the solar irradiance value as

$$\frac{4225.3521W}{m^2} \div 10000 = 4.2W/m^2(1d.p)$$

The values of the solar irradiances at different times were calculated using the same approach as that of the 6:00 local time and is calculated throughout the whole period (6:00 to 18:00hr local time with an interval of 5min). In the same manner, the temperature of the location was recorded in $°C$ and later converted to K using the relation,

$$K = 273.15 + C. \quad (3.3)$$

3.5 Analysis of the data collected

The techniques used to analyze climatological data are classified (Hanks, 1992) as:

(1) Aerodynamic.

(2) Bowen ratio-energy balance (BREB) method.

(3) Combination of the above two methods, and

(4) Empirical.

This research therefore sought to use empirical methods or relationships to explain the dependence of solar radiation on one or more of the environmental parameters.

Using the two separate set-ups, the wireless station Pyranometer and the manual operated Pyranometer, the wireless station saved its data in a propriety binary format and later stored as text file that was imported to Microsoft Excel format. The voltmeter readings from the Pyranometer was manually entered in a text format and saved in Microsoft excel format.

CHAPTER FOUR

RESULTS AND DISCUSSION

4.0 Introduction

In this chapter, the results obtained from the observations of the solar radiation and temperature at the Department of Physics, University of Ghana, Legon together with other atmospheric parameters (including relative humidity) over the study area are presented and thoroughly analyzed to ascertain possible relationships between them.

4.1 Diurnal relationship between temperature and solar radiation with time

Figure 4.1 through to 4.7 represented the diurnal temperature and solar radiation recorded during the period of observation in the month of April from 2/4/2012 to 24/4/2012. The primary vertical axes represent the solar radiation recorded by the Pyranometer (in Watts per square meter) which is proportional to the temperature difference of the Pyranometer's thermopile. The secondary vertical axis represents the Temperature values recorded by the hygro-thermometer corresponding to the outside air temperature (in kelvin). The horizontal axis gives the local time these solar radiation and temperature values were recorded at the observation station.

The first trend that was observed about the graphs was that the solar radiation started from sunrise (6:00 hr), it obtained a maximum value at noon and it virtually shut down at sunset (18:00 hr). The temperature graph showed a different trend. This can be best explained using the following principles: solar radiation directly heats the ground but the ground doesn't immediately warm because of its latent heat capacity.This heat gotten from the ground is used to heat a column of air around it through conduction and its also used to heat cool air above it. At noon, when the sun

reaches its peak height and is directly overhead, because the ground air must first store heat before radiating it to surrounding areas, maximum temperature has not been achieved yet. It actually lags this period of maximum solar heating by several hours which could be seen in the diurnal graphs plotted (Fig. 4.1 to Fig. 4.7). Only when the amount of incoming solar radiation equals the amount of outging radiation does the daily high temperatures occur. The diurnal graphs of Fig. 4.1 to Fig. 4.6 show this particular kind of trend on a normal clear sky day. Fig. 4.7 shows a slight deviation from the normal trend which can be attributed to a specific environmental parameter such as cloud cover. Cloud cover prevents the quantity of solar radiation falling at the particular location.

The seond observable feature that could be noticed is that, the values obtained from the pyranometer readings are in values ranging from as low as 2.8 W/m^2 to as high as 5.6 W/m^2 on the average in the mornings. At noon, where the solar radiation is supposed to be a peak value close to $1000W/m^2$, we get values in the area of 20 W/m^2 to 25 W/m^2 on the average. This low values recorded by the pyranometer might be due to some specific factors which includes: the distance of the pyranometer from the ground (1.3 m), the location of the site close to a building or any obstacle and in this case the obstacle is a tree. A pyranometer recieves direct solar radiation from the whole hemisphere and its inception by an obstacle can reduce the value it records. These obstacles such as a tree located in the vicinity and the building blocks the amount of incoming solar radiation from the sun. Other factors associated with the very low signal input from the pyranometer could be due to environmental factors such as cloud cover and precipitation. This cannot be said of about the values recorded by the pyranometer from the weather station (with a height of 102.4 m) from the wireless weather station where it can be noticed that, values such as low as 7 W/m^2 were recorded in the morinings and values as high as 987 W/m^2 were recorded in the afternoons on the average.

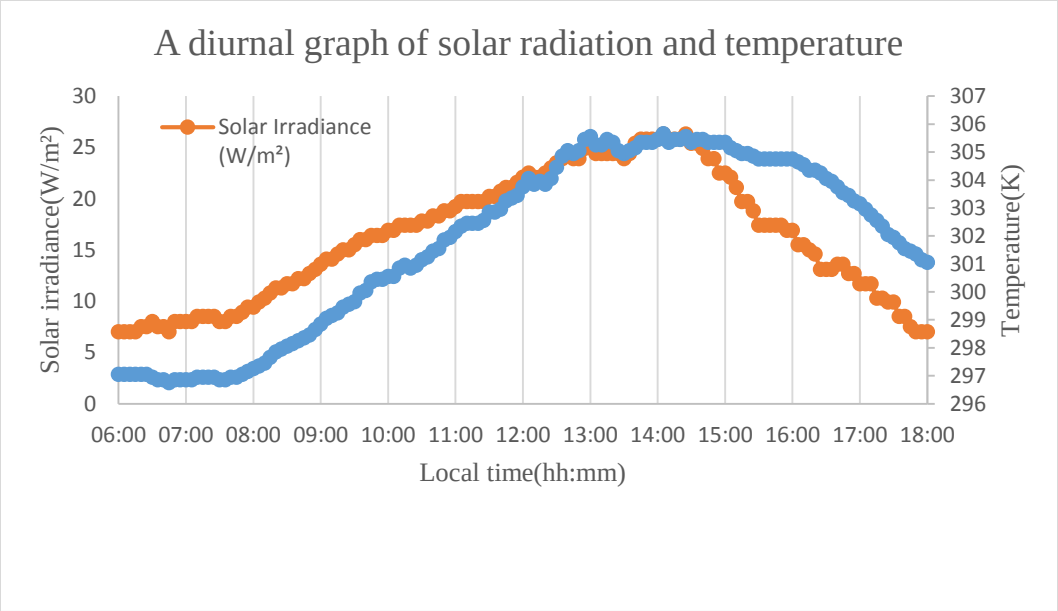

Fig. 4.1: Solar radiation and Temperature recorded on the University of Ghana campus on April 2, 2012.

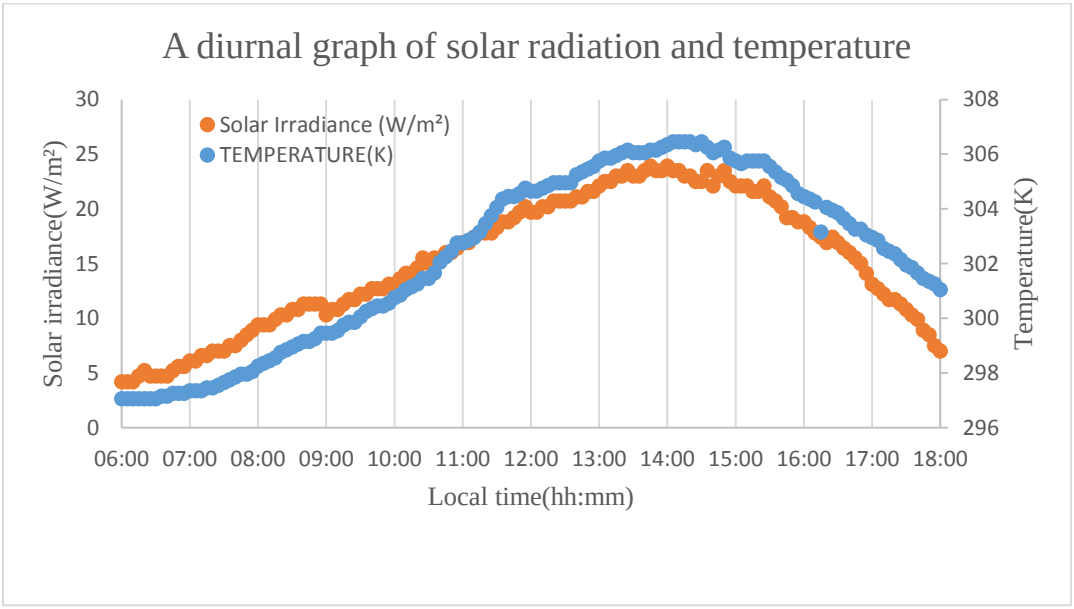

Fig. 4.2: Solar radiation and Temperature recorded on the University of Ghana campus on April 3, 2012.

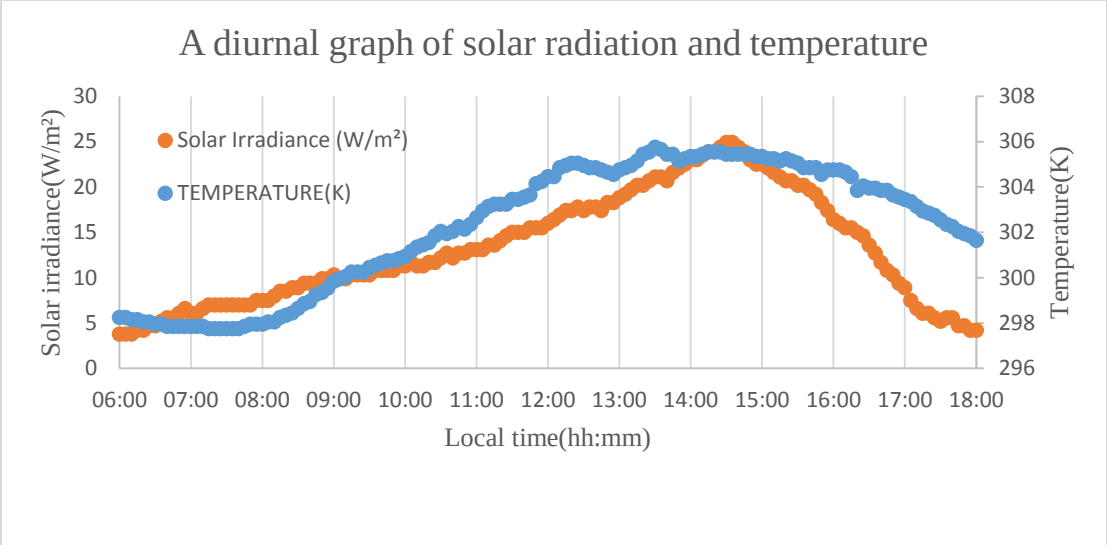

Fig. 4.3: Solar radiation and Temperature recorded on the University of Ghana campus on April 4, 2012.

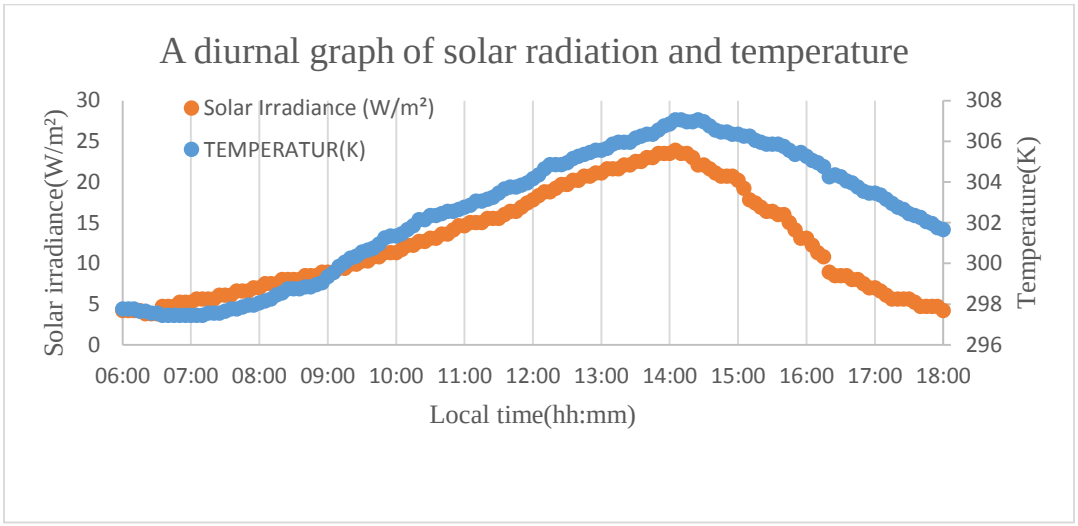

Fig. 4.4: Solar radiation and Temperature recorded on the University of Ghana campus on April 5, 2012.

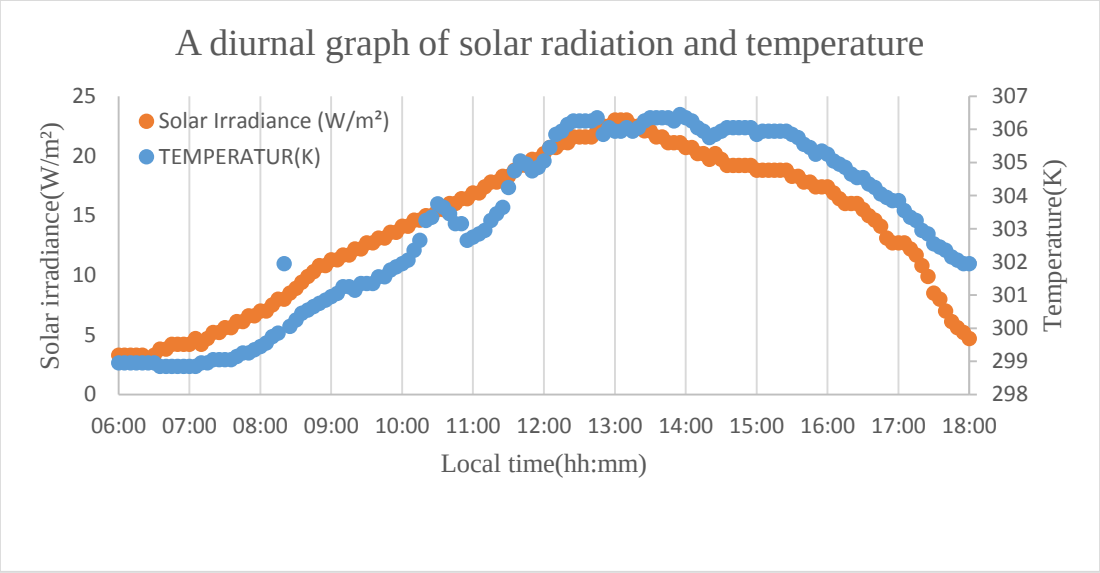

Fig. 4.5: Solar radiation and Temperature recorded on the University of Ghana campus on April 6, 2012.

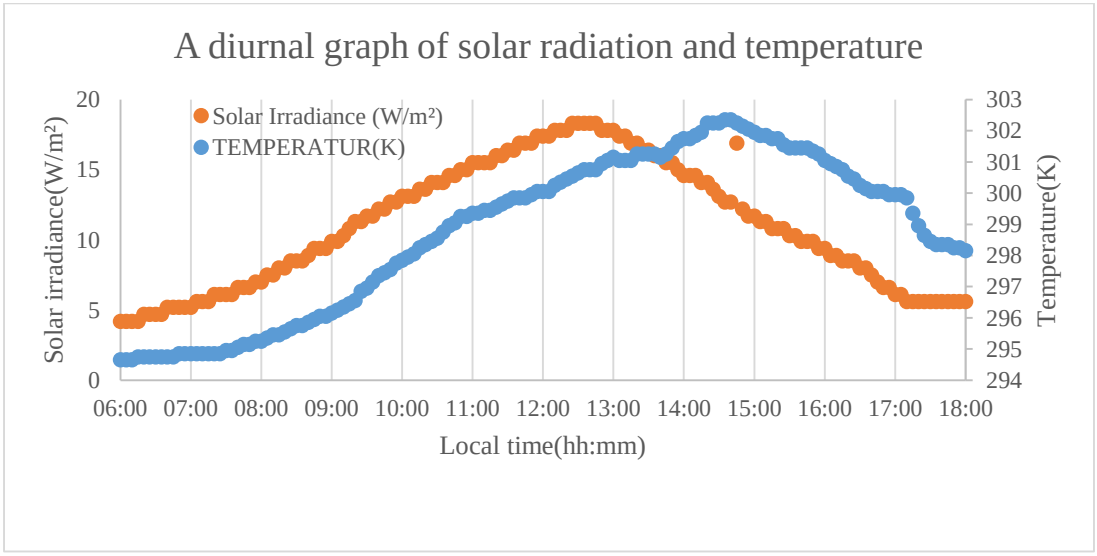

Fig. 4.6: Solar radiation and temperature recorded on the University of Ghana campus on April 11, 2012.

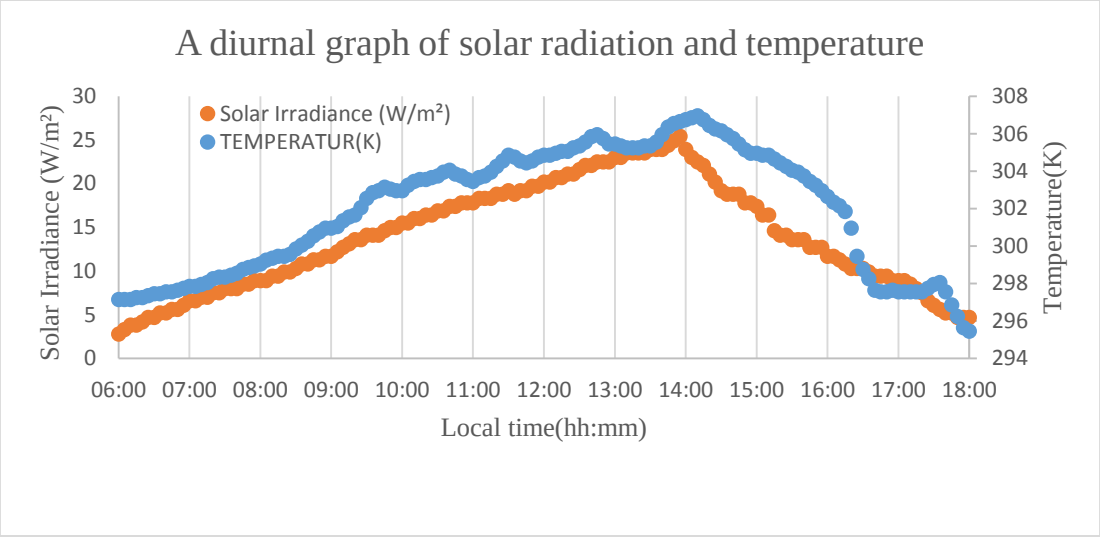

Fig. 4.7: Solar radiation and Temperature recorded on the University of Ghana campus on April 12, 2012.

4.2 Empirical relationships between solar radiation and temperature

Solar radiation is detected by inception and subsequent analysis of the effects of the inception on a receiver (Asogwa *et al*, 2003).

It is therefore clear that radiation amount must be related in some way to temperature. While detailed calculations of atmospheric transfer would be needed to provide the required information for a specific day, it is possible to use statistical regression techniques if only long-term averages are required. The approach adopted by Bajpai and Kalpana (2009) uses linear regression analysis and it forms the basis of this research. The difference in the responsivity value of the Pyranometer at different times enable the graph for a particular day to be split into two sessions namely morning and afternoon session. The data for the morning session was from 6:00 local hr to 11:00 local hr while the data for the evening session is also from 14:00 local hr to 18:00 local hrs. The approach therefore used is obtained from the linear relations as follows;

$$y = ax + b \tag{4.1}$$

Where y = Solar radiation (I) and x = Temperature (T), hence eqn (4.1) becomes;

$$I = aT + b \tag{4.2}$$

Where a and b are constants.

A set of linear equations for the morning and afternoon sessions deduced by analyzing the data read from the pyranometer has been obtained and therefore analyzed with EXCEL.

With the equations obtained by the computer, we form equations using the data from the pyranometer as

$$I_P = a_p T_P + b_p \tag{4.3}$$

And for the wireless

$$I_W = a_w T_W + b_w \tag{4.4}$$

The graphs obtained from the relations of the morning and evening sessions from the pyranometer ($I_P \; and \; T_P$, are the solar radiation and temperature from the pyranometer) and the wireless ($I_W \; and \; T_W$,are the solar radiation and temperature values from the wireless station) are shown. This set of graphs were taken for fourteen different days and compared. The mean solar radiation (I_m) against the mean temperature (T_m) for the experimental set was plotted for the entire duration for which the data was collected.

For the morning session (6:00 to 11:00) on April 2, 2012.

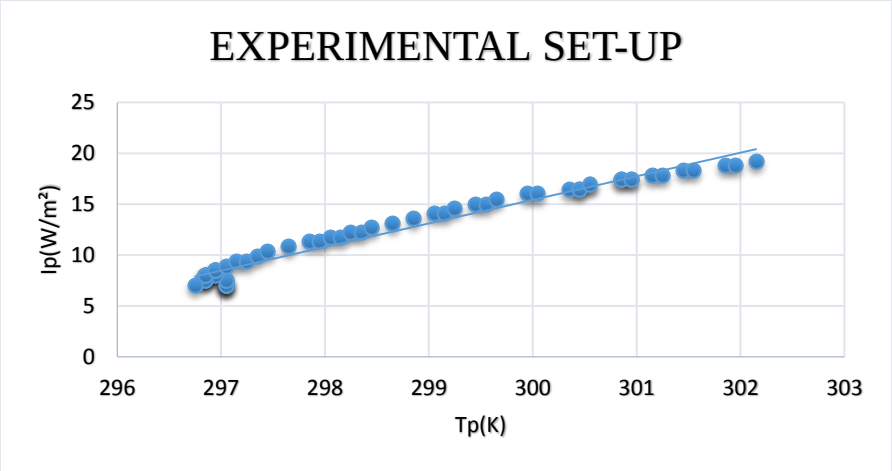

Fig. 4.8: Linear regression analysis of solar radiation (I_p) against temperature (T_p) for the morning session for the experimental set-up recorded on April 2, 2012.

$$\boldsymbol{I_P = 2.3147T_p - 678.99}$$

$$\textbf{Regression coefficient } (\boldsymbol{R^2}) = \boldsymbol{0.97}$$

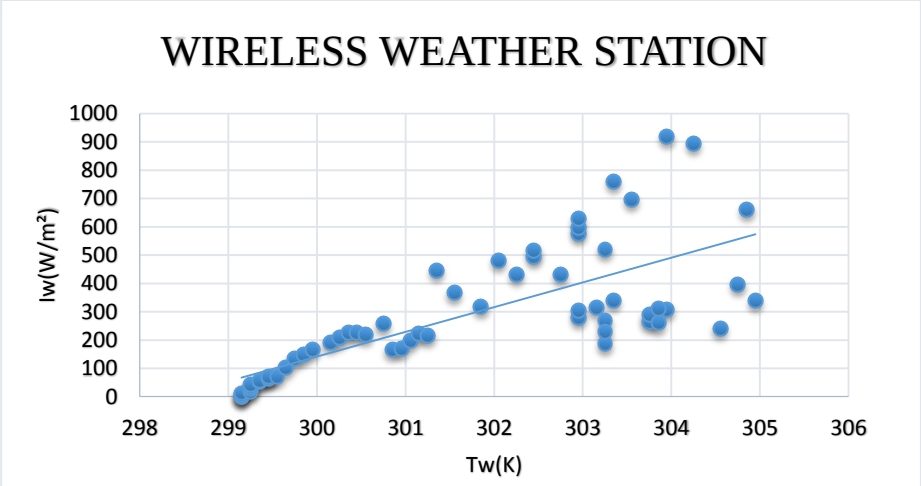

Fig. 4.9: Linear regression analysis of solar radiation (I_w) against temperature (T_w) for the morning session for the wireless weather station recorded on April 2, 2012.

$$\boldsymbol{I_W = 87.293T_W - 26046}$$

$$\textbf{Regression Coefficient } (\boldsymbol{R^2}) = \textbf{0.55}$$

For the evening session (14:00 to 18:00) on April 2, 2012.

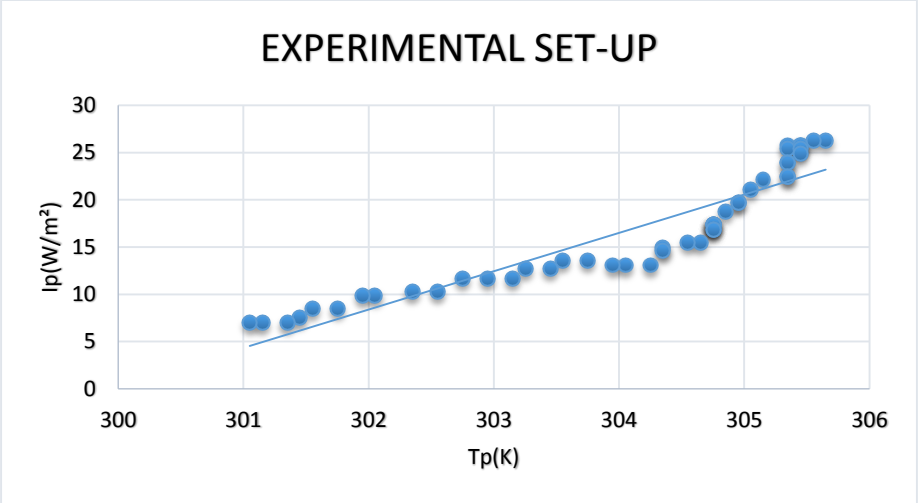

Fig. 4.10: Linear regression analysis of solar radiation (I_p) against temperature (T_p) for the evening session for the experimental set-up recorded on April 2, 2012.

$$\boldsymbol{I_P = 4.0546T_P - 1216.1}$$

$$\textbf{Regression coefficient } (\boldsymbol{R^2}) = \boldsymbol{0.85}$$

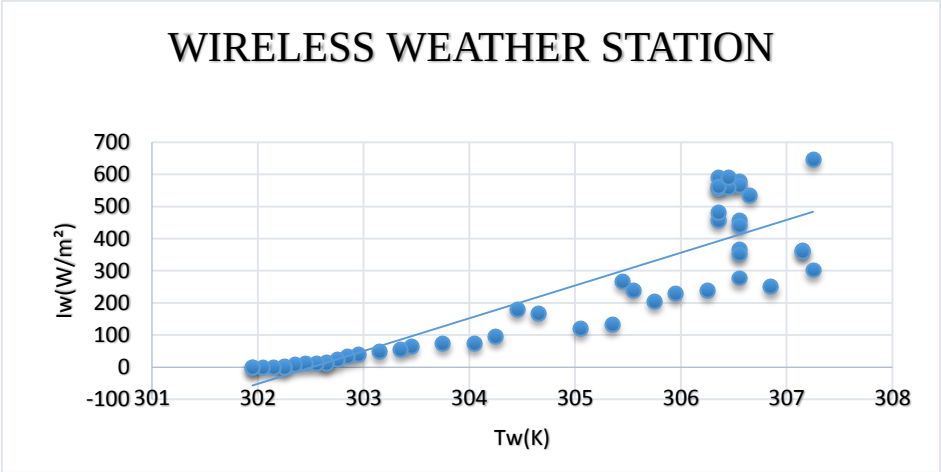

Fig. 4.11: Linear regression analysis of solar radiation (I_w) against temperature (T_w) for the evening session for the wireless weather station recorded on April 2, 2012.

$$\boldsymbol{I_W = 101.93T_W - 30834}$$

$$\textbf{Regression coefficient } (\boldsymbol{R^2}) = \boldsymbol{0.77}$$

For the morning session (6:00 to 11:00) on April 3, 2012.

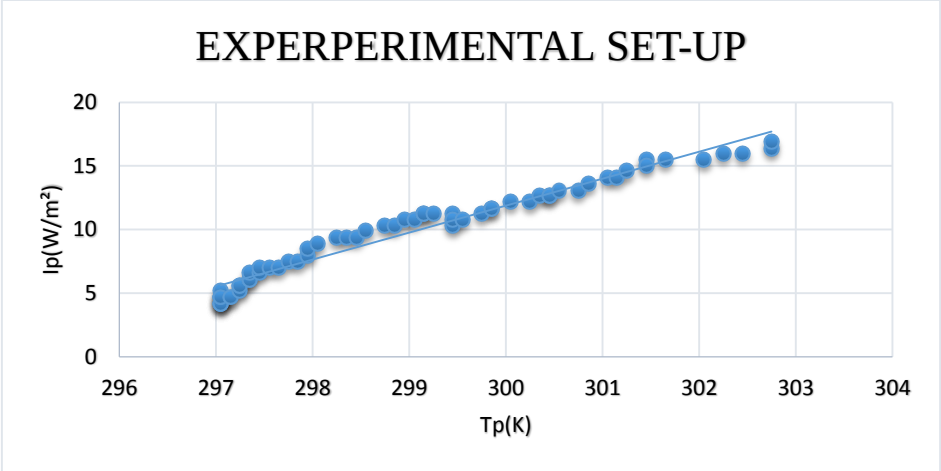

Fig. 4.12: Linear regression analysis of solar radiation (I_p) against temperature (T_p) for the morning session for the experimental set-up recorded on April 3, 2012.

$$\boldsymbol{I_P = 2.1161T_P - 622.96}$$

$$\textbf{Regression Coefficient } (\boldsymbol{R^2}) = \boldsymbol{0.96}$$

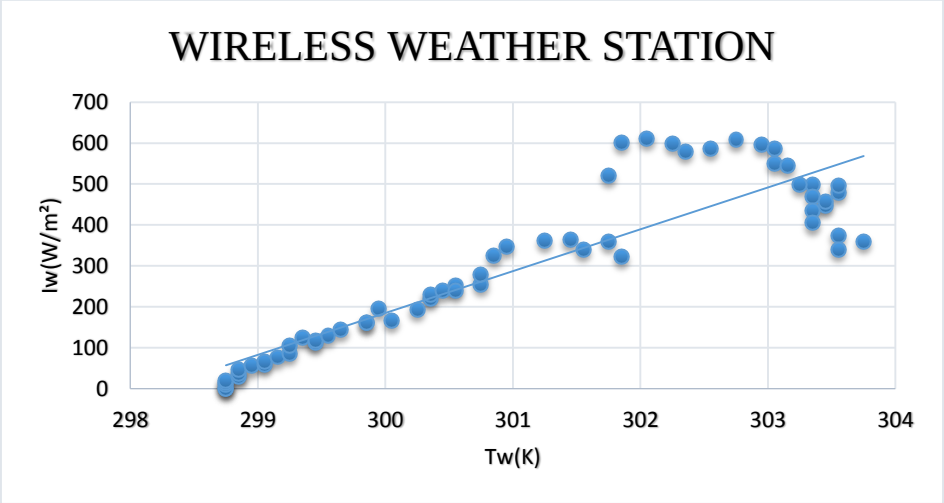

Fig. 4.13: Linear regression analysis of solar radiation (I_w) against temperature (T_w) for the morning session for the wireless weather station recorded on April 3, 2012.

$$\boldsymbol{I_w = 102.29T_w - 30503}$$

$$\textbf{Regression Coefficient } (\boldsymbol{R^2}) = \boldsymbol{0.81}$$

For the evening session (14:00 to 18:00) on April 3, 2012.

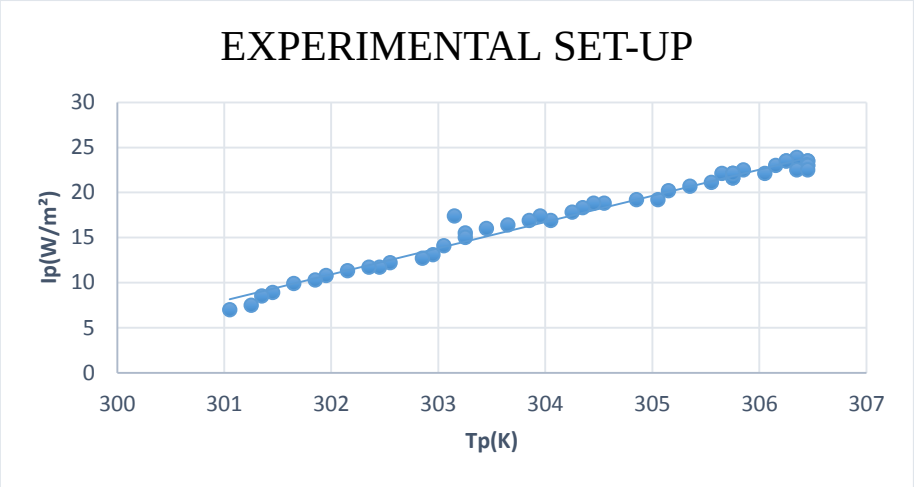

Fig. 4.14: Linear regression analysis of solar radiation (I_p)against temperature (T_p)for the evening session for the experimental set-up recorded on April 3, 2012.

$$\boldsymbol{I_P = 2.9043T_P - 866.16}$$

$$\textbf{Regression Coefficient } (\boldsymbol{R^2}) = \boldsymbol{0.98}$$

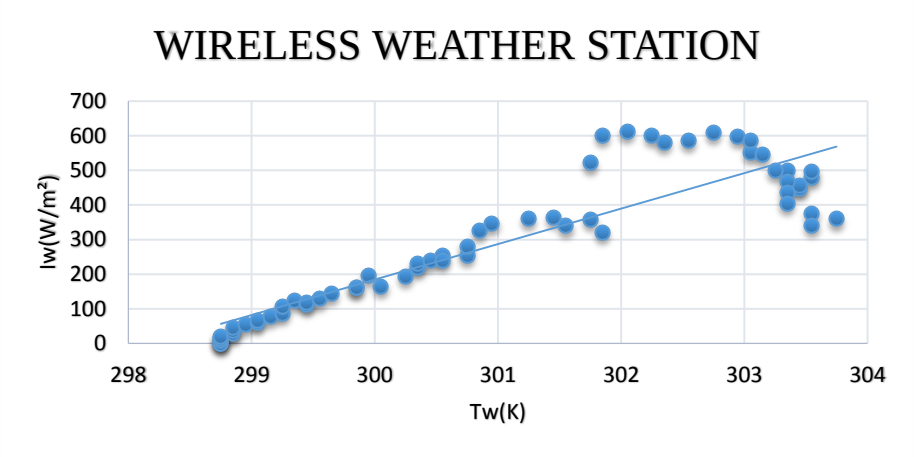

Fig. 4.15: Linear regression analysis of solar radiation (I_w) against temperature (T_w) for the evening session for the weather station recorded on April 3, 2012.

$$\boldsymbol{I_W = 102.29T_W - 30503}$$

$$\textbf{Regression Coefficient } (\boldsymbol{R^2}) = \boldsymbol{0.81}$$

For the morning session (6:00 to 11:00) on April 4, 2012

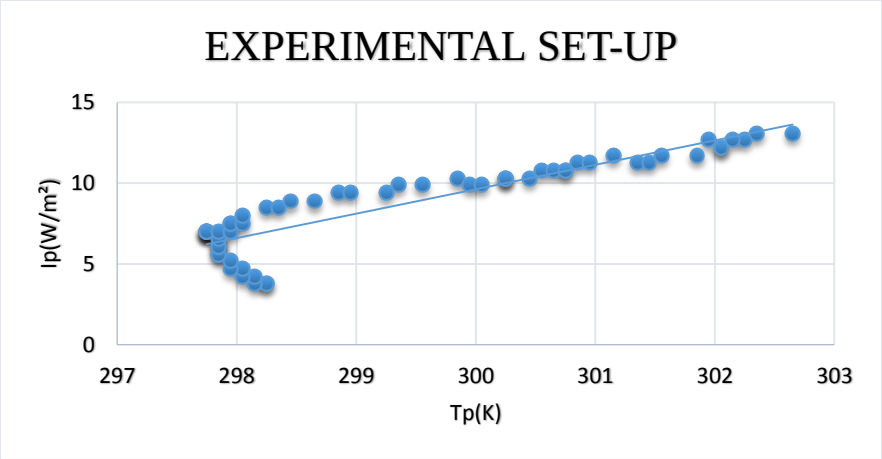

Fig. 4.16: Linear regression analysis of solar radiation (I_p) against temperature T_p) for the morning session for the experimental set-up recorded on April 4, 2012.

$$\boldsymbol{I_P = 1.5085T_P - 442.91}$$

$$\textbf{Regression Coefficient } (\boldsymbol{R^2}) = \boldsymbol{0.81}$$

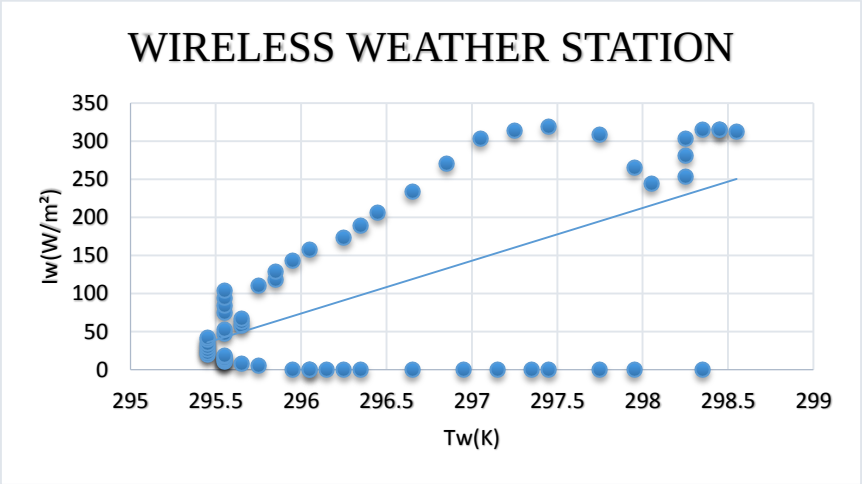

Fig. 4.17: Linear regression analysis of solar radiation (I_w) against temperature (T_w)for the morning session for the wireless weather station recorded on April 4, 2012.

$$\boldsymbol{I_W = 69.303T_W - 20442}$$

$$\textbf{Regression Coefficient } (\boldsymbol{R^2}) = \boldsymbol{0.39}$$

For the evening session (14:00 to 18:00) on April 4, 2012

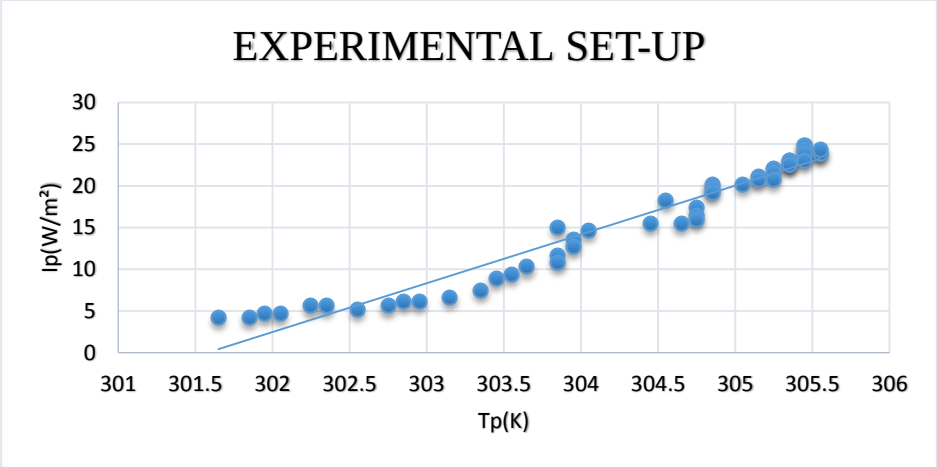

Fig 4.18: Linear regression analysis of solar radiation (I_p) against temperature (T_p) for the evening session for the experimental set-up recorded on April 4, 2012.

$$\boldsymbol{I_P = 5.8531T_P - 1765.2}$$

$$\textbf{Regression Coefficient } (\boldsymbol{R^2}) = \boldsymbol{0.95}$$

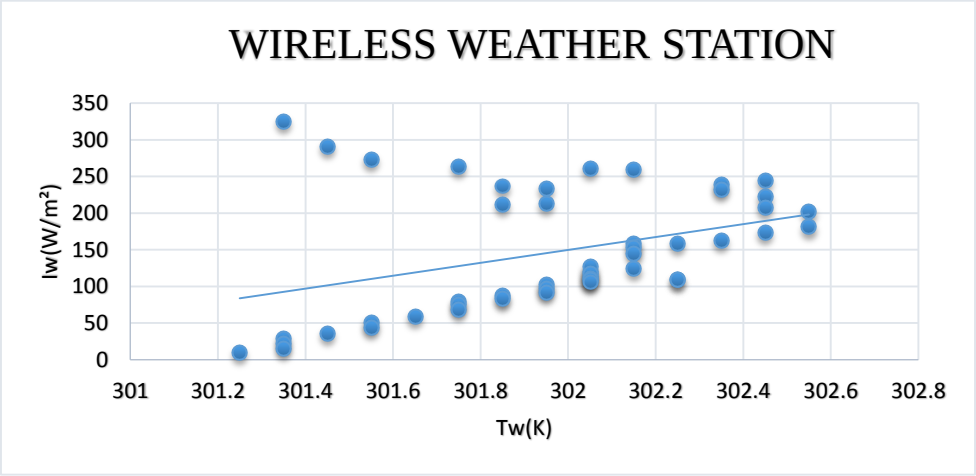

Fig. 4.19: Linear regression analysis of solar radiation (I_w) against temperature (T_w)for the evening session for the wireless weather station recorded on April 4, 2012.

$$\boldsymbol{I_W = 87.929T_W - 26405}$$

$$\textbf{Regression Coefficient } (\boldsymbol{R^2}) = \boldsymbol{0.14}$$

For the morning session (6:00 to 11:00) on April 5, 2012

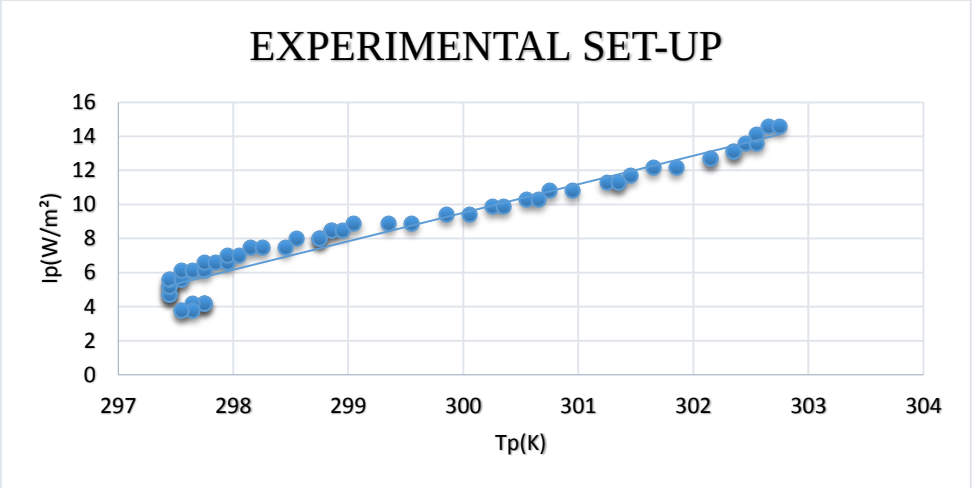

Fig. 4.20: Linear regression analysis of solar radiation (I_p)against temperature (T_p)for the morning session the experimental set-up recorded on April 5, 2012.

$$\boldsymbol{I_P = 1.6745T_P - 492.83}$$

$$\textbf{Regression Coefficient } (\boldsymbol{R^2}) = \boldsymbol{0.95}$$

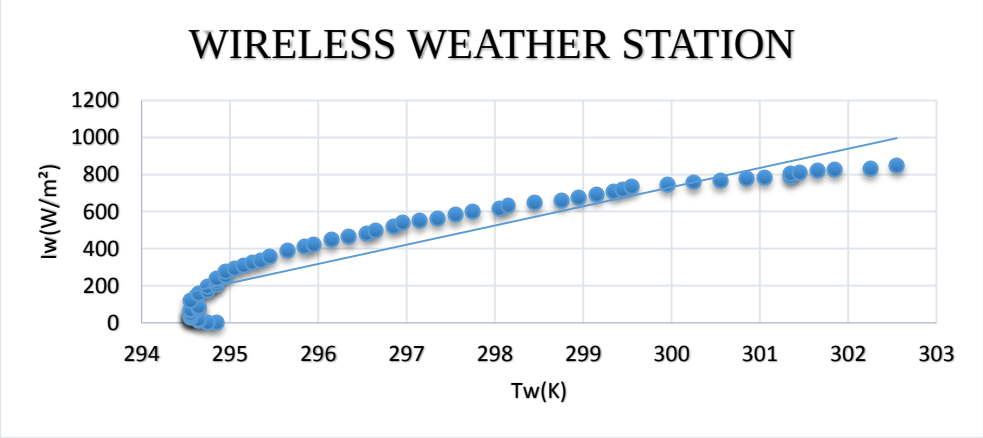

Fig. 4.21: Linear regression analysis of solar radiation (I_w) against temperature (T_w) for the morning session for the wireless weather station recorded on April 5, 2012.

$$\boldsymbol{I_W = 103.5T_W - 30319}$$

$$\textbf{Regression Coefficient } (\boldsymbol{R^2}) = \boldsymbol{0.88}$$

For the evening session (14:00 to 18:00) on April 5, 2012

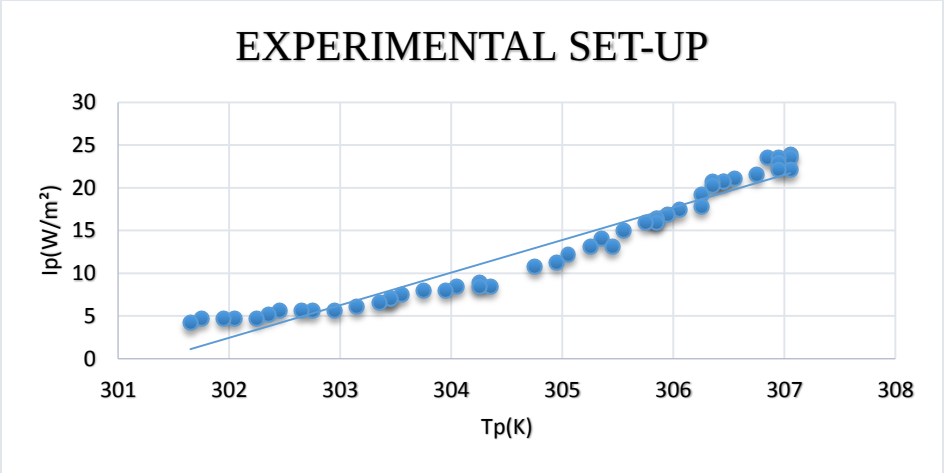

Fig. 4.22: Linear regression analysis of solar radiation (I_p) against temperature (T_p) for the evening session for the experimental set-up recorded on April 5, 2012.

$$\boldsymbol{I_P = 3.8074T_P - 1147.4}$$

$$\textbf{Regression Coefficient } (\boldsymbol{R^2}) = \boldsymbol{0.94}$$

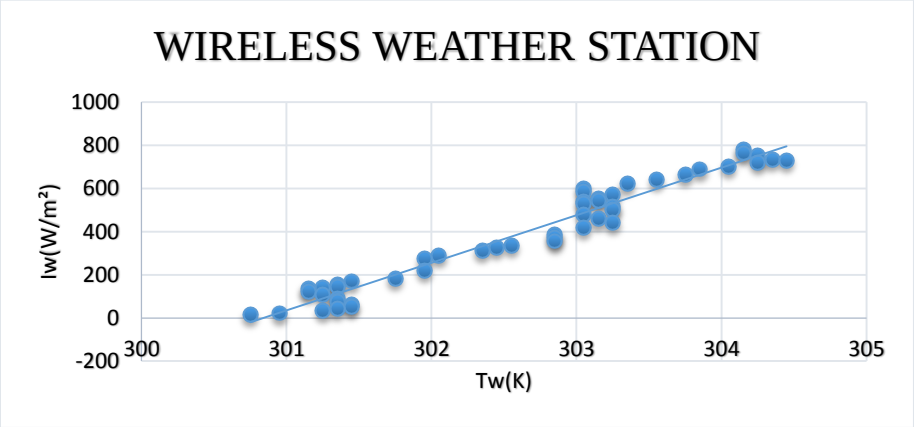

Fig. 4.23: Linear regression analysis of solar radiation (I_w) against temperature (T_w) for the evening session for the wireless weather station recorded on April 5, 2012.

$$\boldsymbol{I_W = 220.38T_W - 66299}$$

$$\textbf{Regression Coefficient } (\boldsymbol{R^2}) = \boldsymbol{0.96}$$

For the morning session (6:00 to 11:00) on April 6, 2012

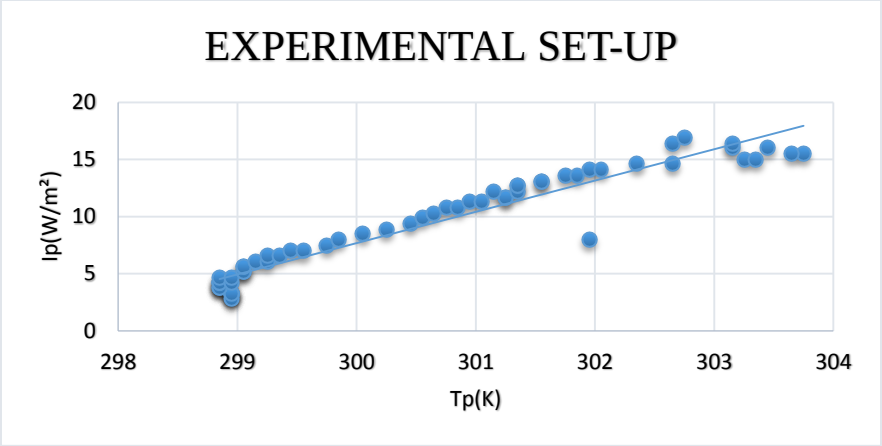

Fig 4.24: Linear regression analysis of solar radiation (I_p)against temperature (T_p)for the morning session for the experimental set-up recorded on April 6, 2012

$$\boldsymbol{I_P = 2.7381T_P - 813.75}$$

$$\textbf{Regression Coefficient } (\boldsymbol{R^2}) = \boldsymbol{0.93}$$

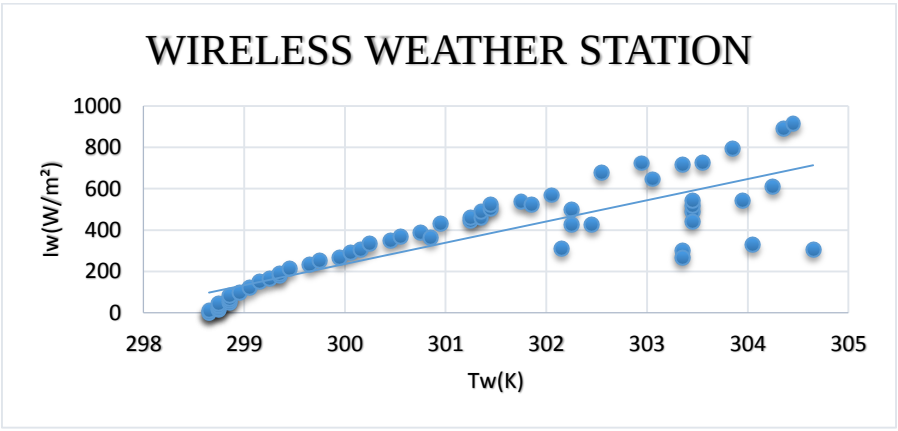

Fig. 4.25: Linear regression analysis of solar radiation (I_w) against temperature (T_w) for the morning session for wireless weather station recorded on April 6, 2012.

$$\boldsymbol{I_W = 102.82T_W - 30612}$$

$$\textbf{Regression Coefficient } (\boldsymbol{R^2}) = \boldsymbol{0.71}$$

For the evening session (14:00 to 18:00) on April 6, 2012

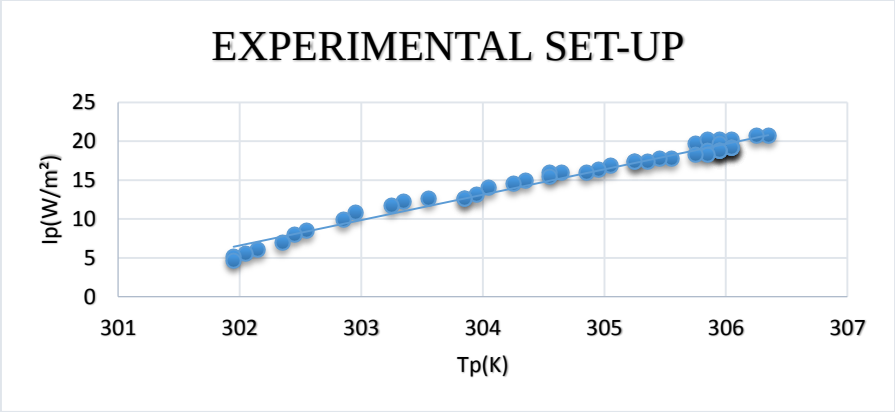

Fig. 4.26: Linear regression analysis of solar radiation (I_p)against temperature (T_p) for the evening session for the experimental set-up recorded on April 6, 2012.

$$\boldsymbol{I_P = 3.2649T_P - 979.42}$$

$$\textbf{Regression Coefficient } (\boldsymbol{R^2}) = \boldsymbol{0.97}$$

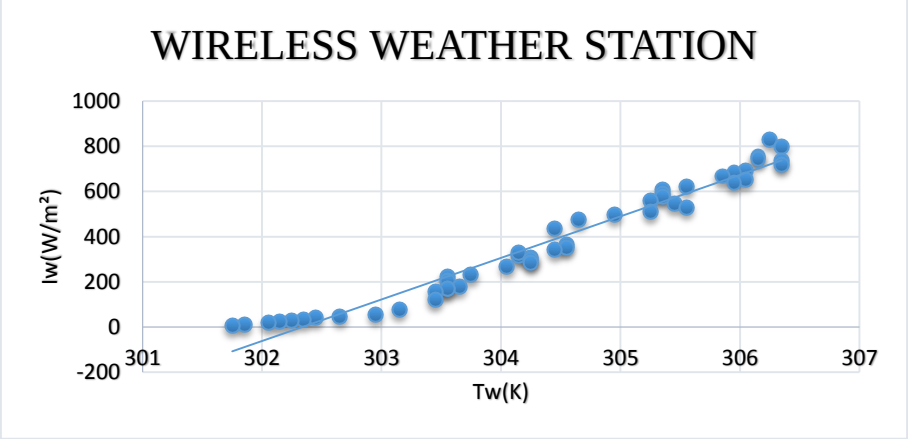

Fig. 4.27: Linear regression analysis of solar radiation (I_w) against temperature (T_w) for the evening session for the wireless weather station recorded on April 6, 2012.

$$\boldsymbol{I_W = 183.81T_W - 55572}$$

$$\textbf{Regression Coefficient } (\boldsymbol{R^2}) = \boldsymbol{0.96}$$

For the morning session (6:00 to 11:00) on April 11, 2012

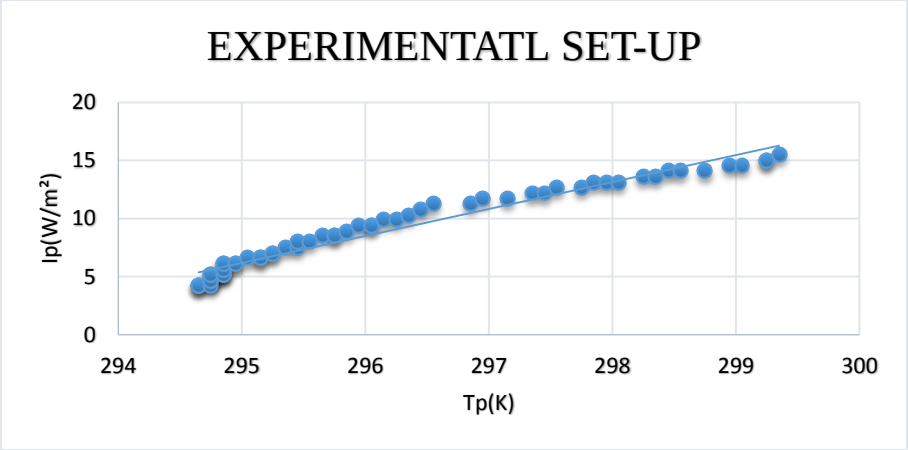

Fig. 4.28: Linear regression analysis for solar radiation (I_p) against temperature (T_p) for the morning session for the experimental set-up recorded on April 11, 2012.

$$\boldsymbol{I_P = 2.3198T_P - 678.14}$$

$$\textbf{Regression Coefficient } (\boldsymbol{R^2}) = \boldsymbol{0.96}$$

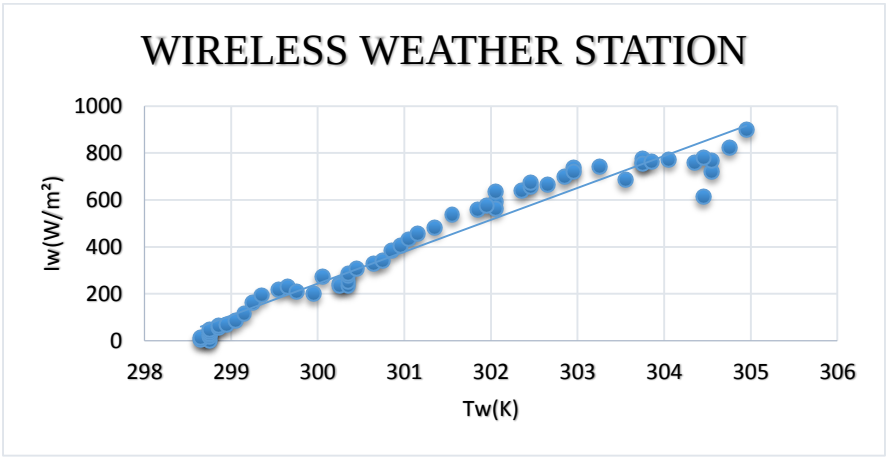

Fig. 4.29: Linear regression analysis for solar radiation (I_w) against temperature (T_w)for the morning session for the wireless weather station recorded on April 11, 2012.

$$\boldsymbol{I_W = 136.22T_W - 40623}$$

$$\textbf{Regression Coefficient } (\boldsymbol{R^2}) = \boldsymbol{0.95}$$

For the evening session (14:00 to 18:00) on April 11, 2012

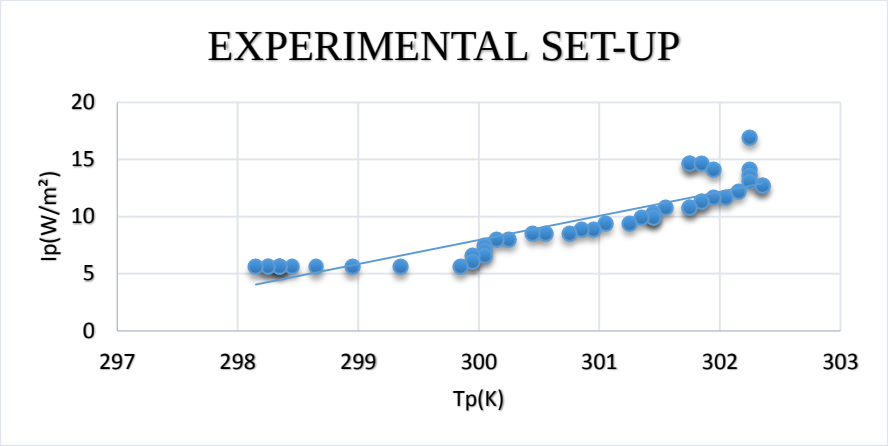

Fig. 4.30: Linear regression analysis for solar radiation (I_p) against temperature (T_p) for the evening session for the experimental set-up recorded on April 11, 2012.

$$\boldsymbol{I_P = 2.1098T_P - 625}$$

$$\textbf{Regression Coefficient } (\mathbf{R^2}) = \mathbf{0.81}$$

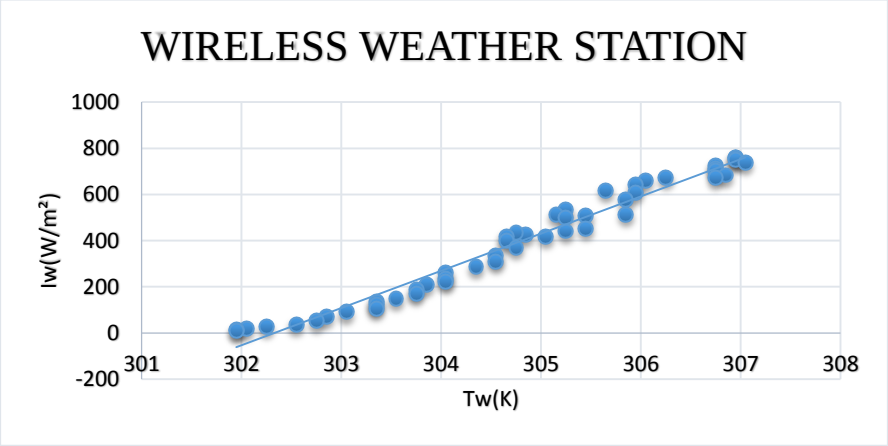

Fig. 4.31: Linear regression analysis for solar radiation (I_w) against temperature (T_w) for the evening session for the wireless weather station recorded on April 11, 2012.

$$\boldsymbol{I_W = 161.31T_W - 48769}$$

$$\textbf{Regression Coefficient } (\boldsymbol{R^2}) = \mathbf{0.97}$$

For the morning session (6:00 to 11:00) on April 12, 2012

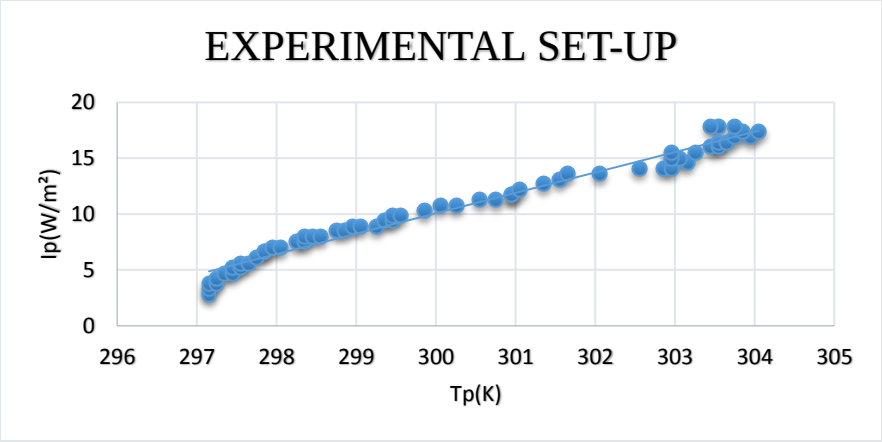

Fig. 4.32: Linear regression analysis of solar radiation (I_p) against temperature (T_p) for the morning session for the experimental set-up recorded on April 12, 2012.

$$\boldsymbol{I_P = 1.8273T_P - 538.11}$$

$$\textbf{Regression Coefficient } (\mathbf{R^2}) = \mathbf{0.97}$$

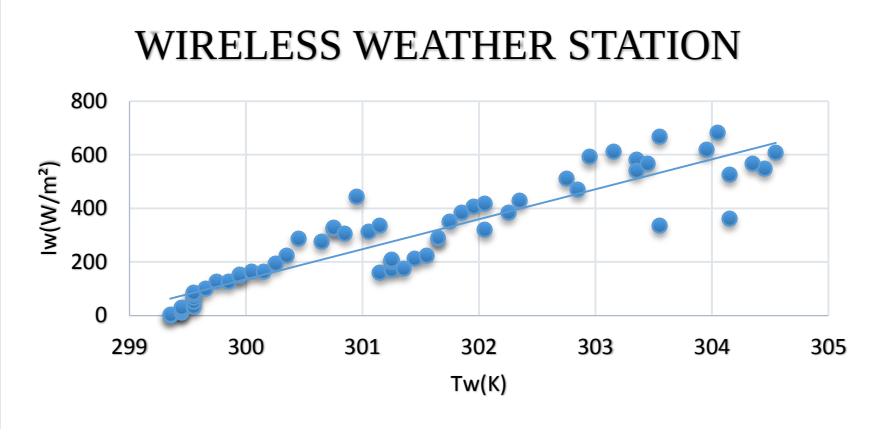

Fig. 4.33: Linear regression analysis of solar radiation (I_w) against temperature (T_w) for the morning session for the wireless weather station recorded on April 12, 2012.

$$\boldsymbol{I_W = 11164T_W - 33356}$$

$$\textbf{Regression Coefficient } (\boldsymbol{R^2}) = \mathbf{0.83}$$

For the evening session (14:00 to 18:00) on April 12, 2012

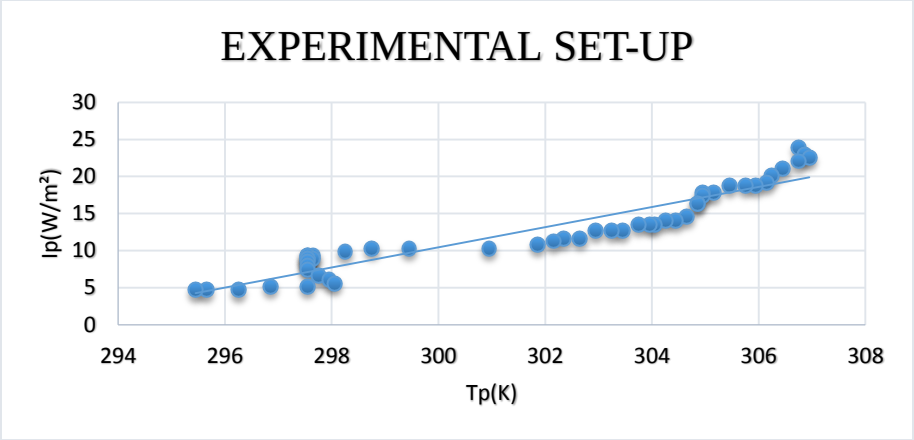

Fig. 4.34: Linear regression analysis of solar radiation (I_p) against temperature (T_p) for the evening session for the experimental set-up recorded on April 12, 2012.

$$\boldsymbol{I_P = 1.3569T_P - 369.64}$$

$$\textbf{Regression Coefficient} \boldsymbol{R^2 = 0.89}$$

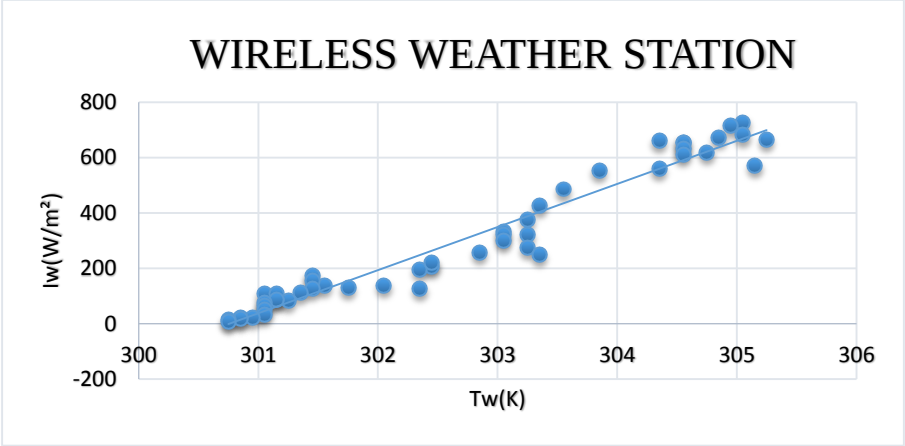

Fig. 4.35: Linear regression analysis of solar radiation (I_w) against temperature (T_w) for the evening session for the wireless weather station recorded on April 12, 2012.

$$\boldsymbol{I_W = 155.47T_W - 46758}$$

$$\textbf{Regression Coefficient } \boldsymbol{(R^2) = 0.95}$$

For the morning session (6:00 to 11:00) on April 13, 2012

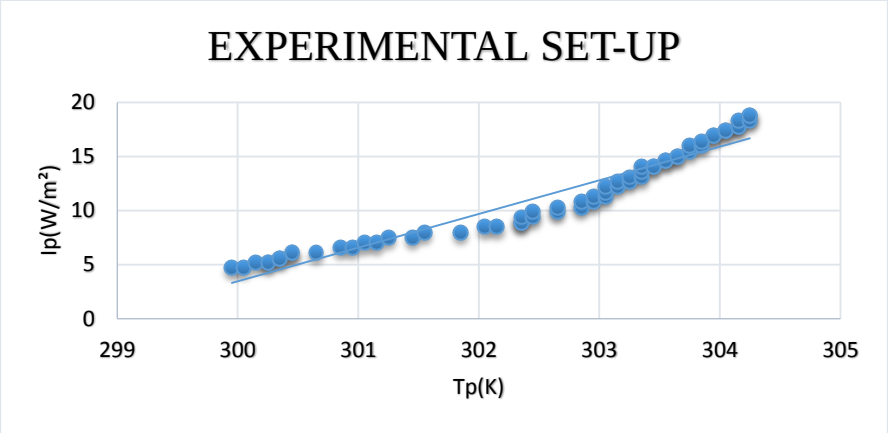

Fig. 4.36: Linear regression analysis of solar radiation (I_p) against temperature (T_p) for the morning session for the experimental set-up recorded on April 13, 2012.

$$\boldsymbol{I_P = 3.1061T_P - 928.35}$$

$$\textbf{Regression Coefficient } (\boldsymbol{R^2}) = \boldsymbol{0.92}$$

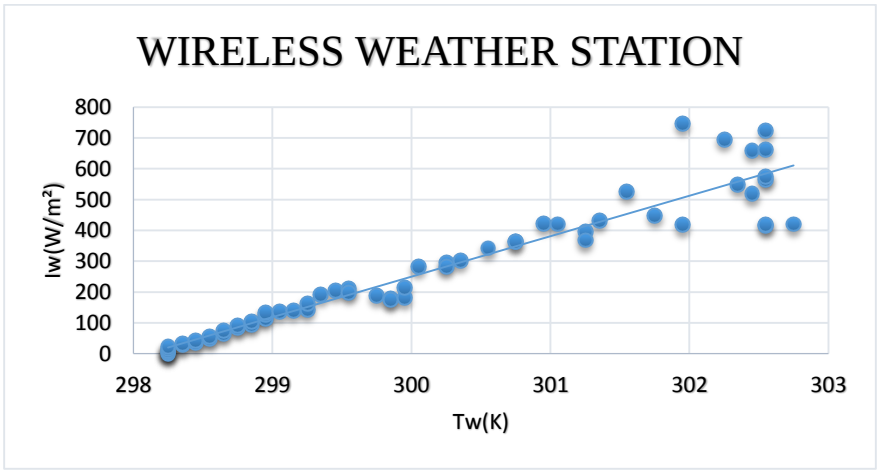

Fig. 4.37: Linear regression analysis of solar radiation (I_w) against temperature (T_w) for the morning session for the wireless weather station recorded on April 13, 2012.

$$\boldsymbol{I_W = 131.42T_W - 39175}$$

$$\textbf{Regression Coefficient } (\boldsymbol{R^2}) = \boldsymbol{0.91}$$

For the evening session (14:00 to 18:00) on April 13, 2012

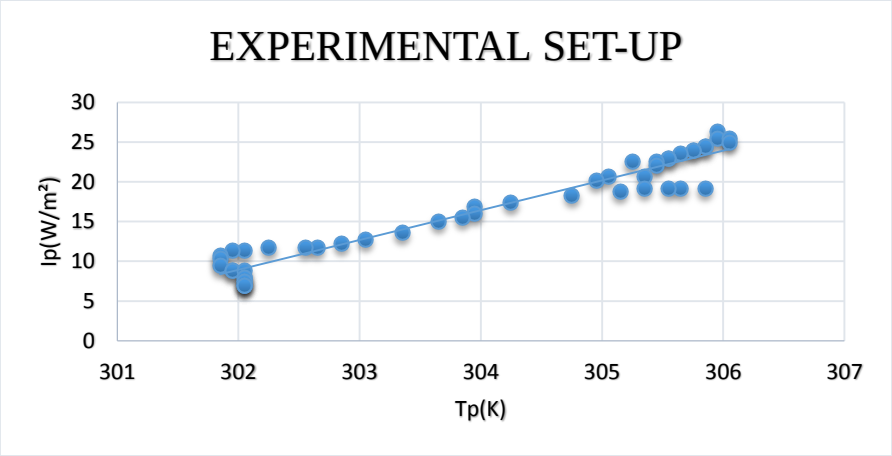

Fig. 4.38: Linear regression analysis of solar radiation (I_p) against temperature (T_p) for the evening session for the experimental set-up recorded on April 13, 2012.

$$\boldsymbol{I_P = 3.7426T_P - 1121.3}$$

$$\textbf{Regression Coefficient } (\boldsymbol{R^2}) = \boldsymbol{0.93}$$

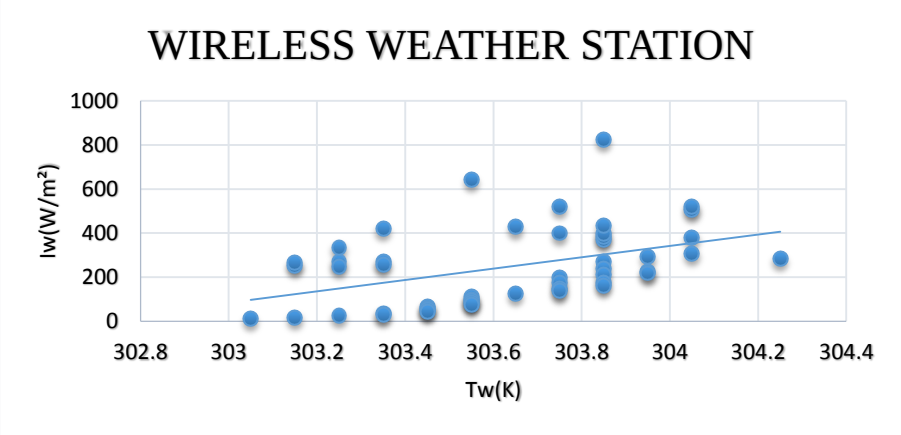

Fig. 4.39: Linear regression analysis of solar radiation (I_w) against temperature (T_w) for the evening session for the wireless weather station recorded on April 13, 2012.

$$\boldsymbol{I_W = 257.74T_W - 78011}$$

$$\textbf{Regression Coefficient } (\boldsymbol{R^2}) = \boldsymbol{0.18}$$

For the morning session (6:00 to 11:00) on April 16, 2012

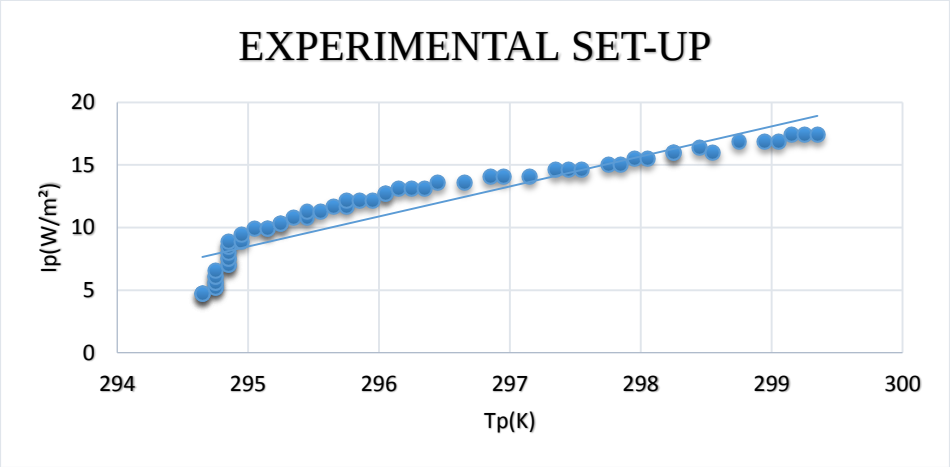

Fig. 4.40: Linear regression analysis of solar radiation (I_p) against temperature (T_p) for the morning session for the experimental set-up recorded on April 16, 2012.

$$\boldsymbol{I_P = 2.3992T_P - 699.27}$$

$$\textbf{Regression Coefficient } (\boldsymbol{R^2}) = \boldsymbol{0.86}$$

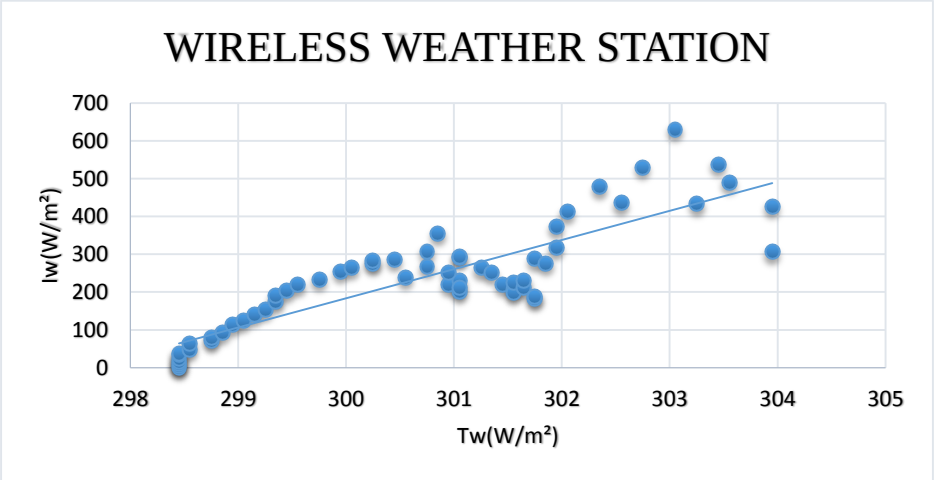

Fig. 4.41: Linear regression analysis of solar radiation (I_w) against temperature (T_w) for the morning session for the wireless weather station recorded on April 16, 2012.

$$\boldsymbol{I_w = 77.127T_w - 22954}$$

$$\textbf{Regression Coefficient } (\boldsymbol{R^2}) = \boldsymbol{0.74}$$

For the evening session (14:00 to 18:00) on April 16, 2012

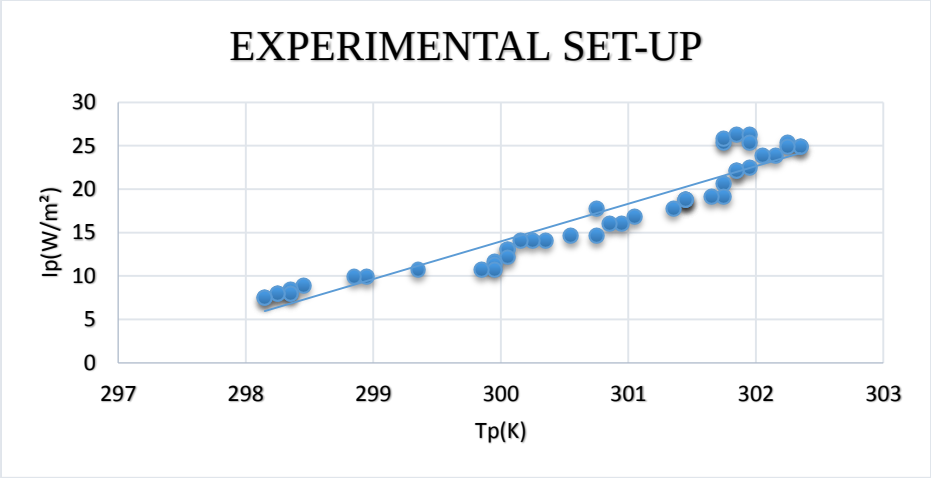

Fig. 4.42: Linear regression analysis of solar radiation (I_p) against temperature (T_p) for the evening session for the experimental set-up recorded on April 16, 2012.

$$\boldsymbol{I_P = 4.3345T_P - 1286.4}$$

$$\textbf{Regression Coefficient } (\boldsymbol{R^2}) = \boldsymbol{0.90}$$

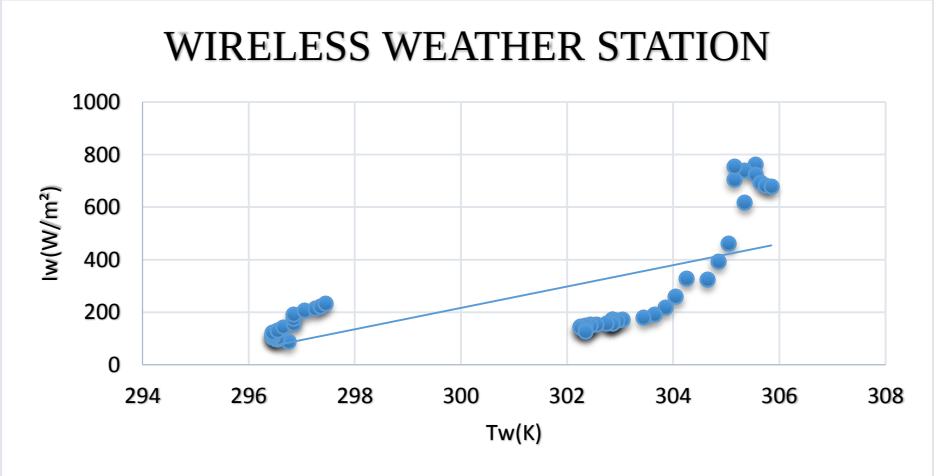

Fig. 4.43: Linear regression analysis of solar radiation (I_w) against temperature (T_w) for the evening session for the wireless weather station recorded on April 16, 2012.

$$\boldsymbol{I_W = 40.729T_W - 12002}$$

$$\textbf{Regression Coefficient } (\boldsymbol{R^2}) = \boldsymbol{0.42}$$

For the morning session (6:00 to 11:00) on April 17, 2012

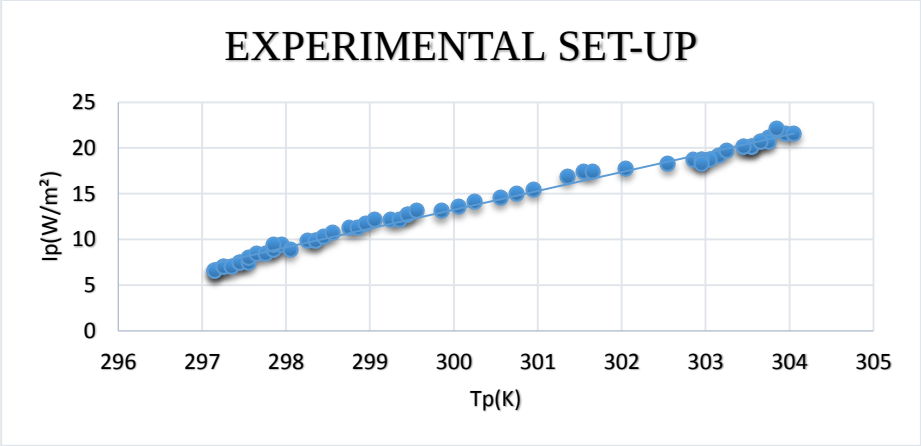

Fig. 4.44: Linear regression analysis of solar radiation (I_p) against temperature (T_p) for the morning session the experimental set-up recorded on April 17, 2012.

$$\boldsymbol{I_P = 2.0602T_P - 604.79}$$

$$\textbf{Regression Coefficient } (\boldsymbol{R^2}) = \boldsymbol{0.99}$$

For the evening session (14:00 to 18:00) on April 17, 2012

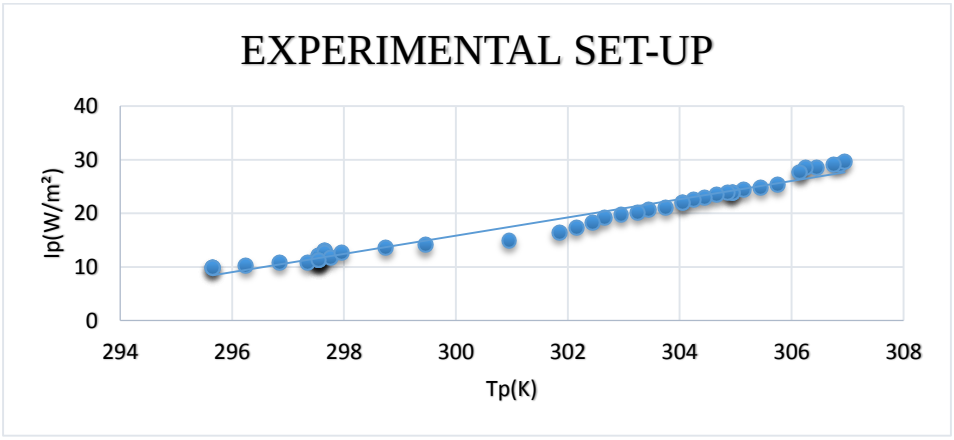

Fig. 4.45: Linear regression analysis of solar radiation (I_p) against temperature (T_p) for the evening session the experimental set-up recorded on April 17, 2012.

$$\boldsymbol{I_P = 1.6997T_P - 494.06}$$

$$\textbf{Regression Coefficient } (\boldsymbol{R^2}) = \boldsymbol{0.97}$$

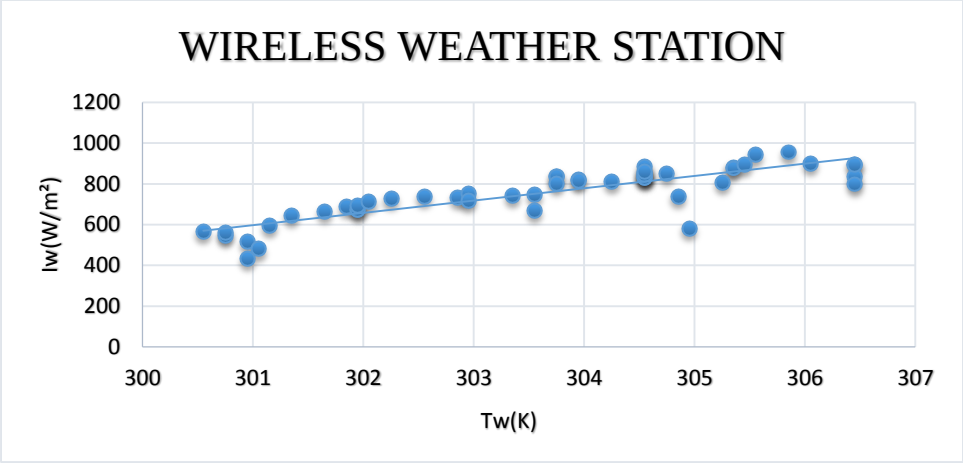

Fig. 4.46: Linear regression analysis of solar radiation (I_w) against temperature (T_w) for the evening session for the wireless weather station recorded on April 17, 2012.

$$\boldsymbol{I_W = 60.375T_w - 17576}$$

$$\textbf{Regression Coefficient } (\boldsymbol{R^2}) = \boldsymbol{0.72}$$

For the morning session (6:00 to 11:00) on April 19, 2012

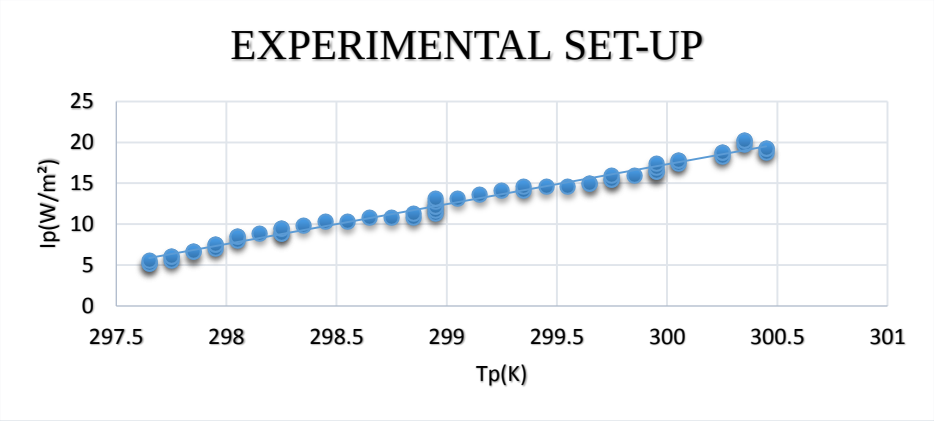

Fig. 4.47: Linear regression analysis of solar radiation (I_p) against temperature (T_p) for the morning session for the experimental set-up recorded on April 19, 2012.

$$\boldsymbol{I_P = 4.879T_P - 1446.4}$$

$$\textbf{Regression Coefficient } (\boldsymbol{R^2}) = \boldsymbol{0.99}$$

For the evening session (14:00 to 18:00) on April 19, 2012

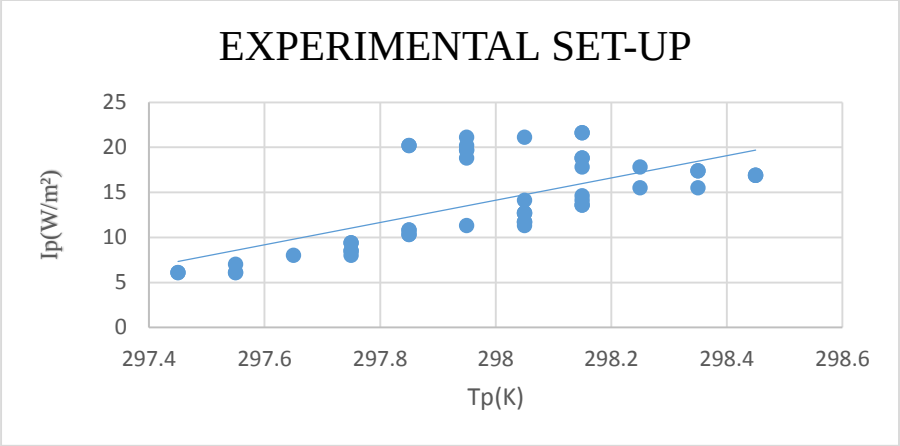

Fig. 4.48: Linear regression analysis of solar radiation (I_p) against temperature (T_p) for the evening session for the experimental set-up recorded on April 19, 2012.

$$\boldsymbol{I_p = 12.942T_p - 3842.5}$$

$$\textbf{Regression Coefficient } (\boldsymbol{R^2}) = \boldsymbol{0.45}$$

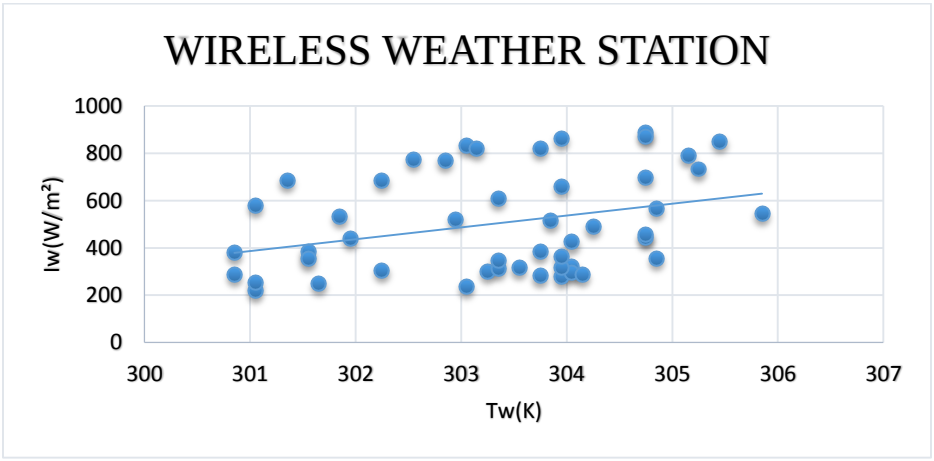

Fig. 4.49: Linear regression analysis of solar radiation (I_w) against temperature (T_w) for the evening session for the wireless weather station recorded on April 19, 2012.

$$\boldsymbol{I_W = 50.074T_W - 14686}$$

$$\textbf{Regression Coefficient } (\boldsymbol{R^2}) = \boldsymbol{0.10}$$

For the morning session (6:00 to 11:00) on April 20, 2012

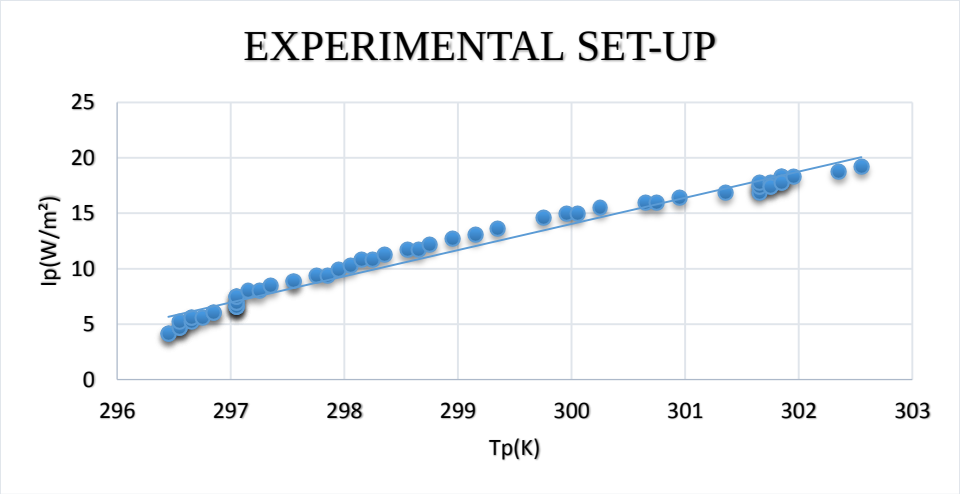

Fig. 4.50: Linear regression analysis of solar radiation (I_p) against temperature (T_p) for the morning session for the experimental set-up recorded on April 20, 2012.

$$\boldsymbol{I_P = 2.3588T_P - 693.6}$$

$$\textbf{Regression Coefficient } (\boldsymbol{R^2}) = \boldsymbol{0.98}$$

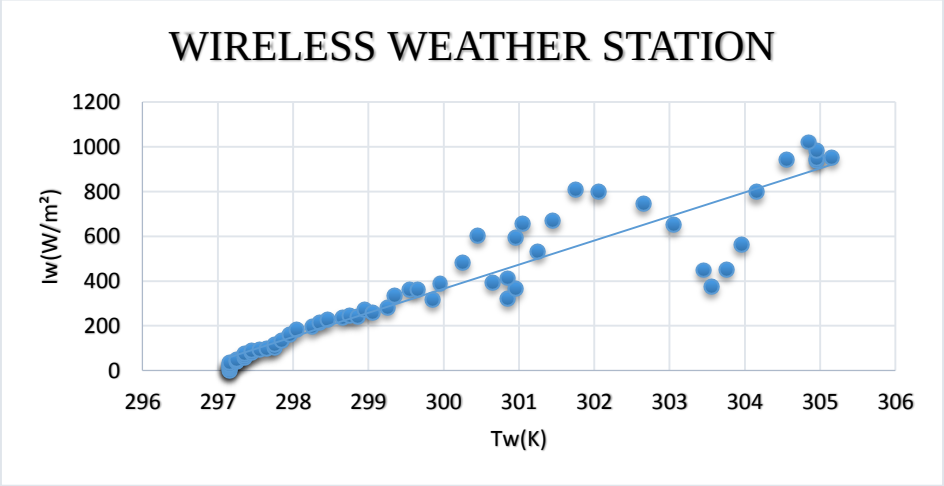

Fig. 4.51: Linear regression analysis of solar radiation (I_w) against temperature (T_w) for the morning session for the wireless weather station recorded on April 20, 2012.

$$\boldsymbol{I_W = 107.65T_W - 31928}$$

$$\textbf{Regression Coefficient } (\boldsymbol{R^2}) = \boldsymbol{0.87}$$

For the evening session (14:00 to 18:00) on April 20, 2012

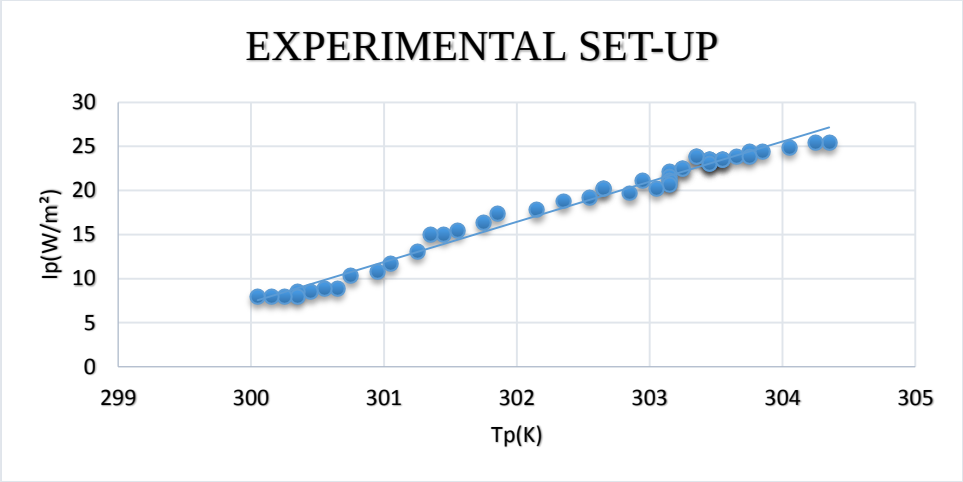

Fig. 4.52: Linear regression analysis of solar radiation (I_p) against temperature (T_p) for the evening session for the experimental set-up recorded on April 20, 2012.

$$\boldsymbol{I_P = 4.5526T_P - 1358.5}$$

$$\textbf{Regression Coefficient } (\boldsymbol{R^2}) = \boldsymbol{0.98}$$

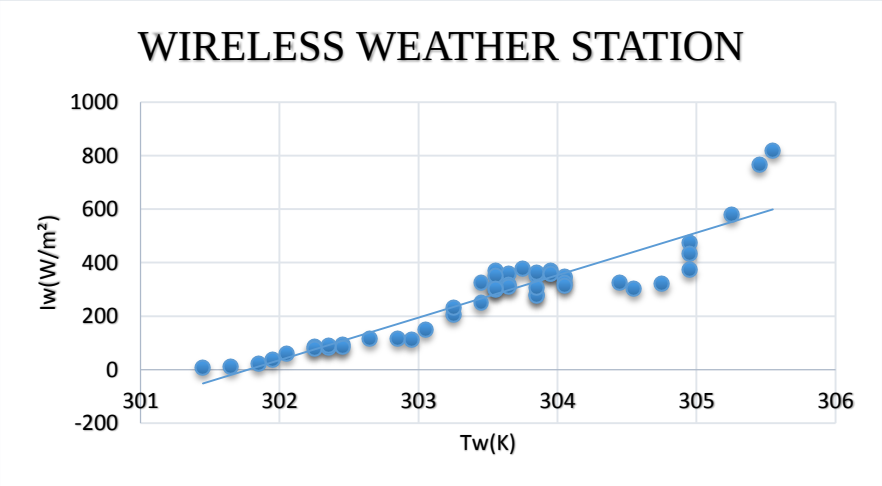

Fig. 4.53: Linear regression analysis of solar radiation (I_w) against temperature (T_w) for the evening session for the wireless weather station recorded on April 20, 2012.

$$\boldsymbol{I_W = 158.69T_W - 47890}$$

$$\textbf{Regression Coefficient } (\boldsymbol{R^2}) = \boldsymbol{0.85}$$

For the morning session (6:00 to 11:00) on April 23, 2012

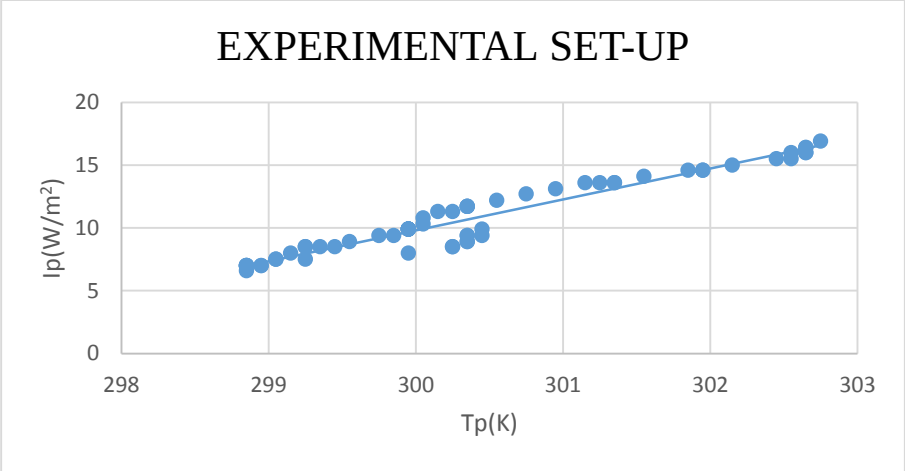

Fig. 4.54: Linear regression analysis of solar radiation (I_p) against temperature (T_p) for the morning session for the experimental set-up recorded on April 23, 2012.

$$\boldsymbol{I_p = 2.4675T_p - 730.45}$$

$$\textbf{Regression Coefficient } (\boldsymbol{R^2}) = \boldsymbol{0.94}$$

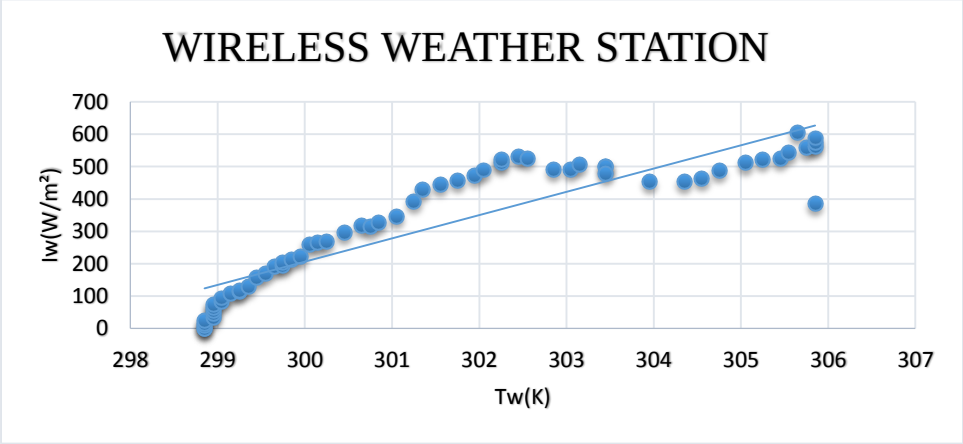

Fig. 4.55: Linear regression analysis of solar radiation (I_w) against temperature (T_w) for the morning session for the wireless weather station recorded on April 23, 2012.

$$\boldsymbol{I_W = 71.914T_W - 21368}$$

$$\textbf{Regression Coefficient } (\boldsymbol{R^2}) = \boldsymbol{0.81}$$

For the evening session (14:00 to 18:00) on April 23, 2012

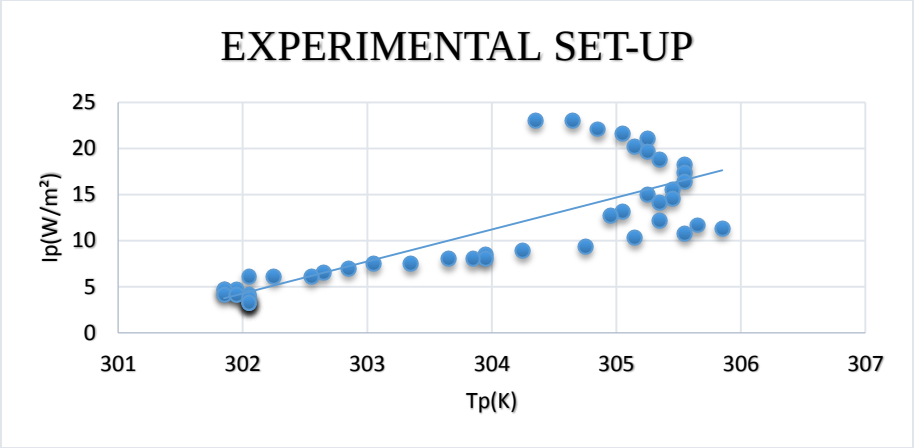

Fig. 4.56: Linear regression analysis of solar radiation (I_p) against temperature (T_p) for the evening session for the experimental set-up recorded on April 23, 2012.

$$\boldsymbol{I_P = 3.4728T_P - 1044.5}$$

$$\textbf{Regression Coefficient } (\boldsymbol{R^2}) = \boldsymbol{0.67}$$

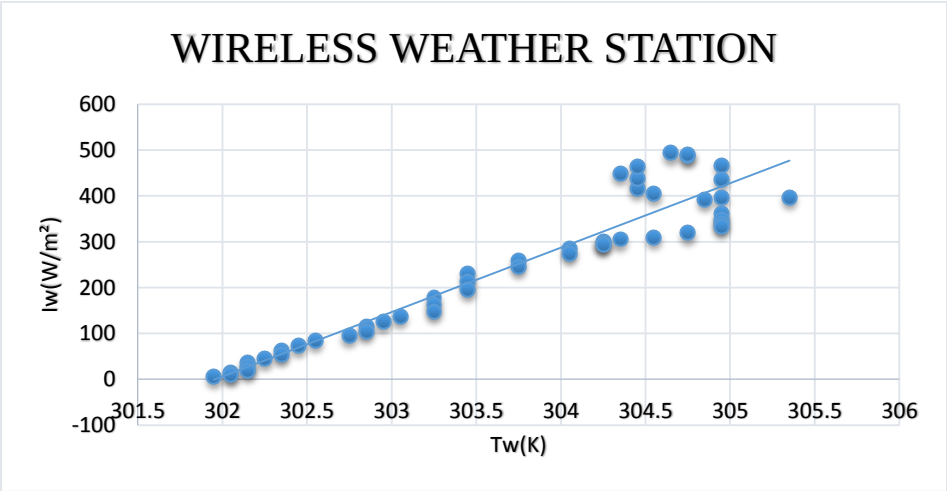

Fig. 4.57: Linear regression analysis of solar radiation (I_w) against temperature (T_w) for the evening session for the wireless weather station recorded on April 23, 2012.

$$\boldsymbol{I_W = 140.63T_W - 42464}$$

$$\textbf{Regression Coefficient } (\boldsymbol{R^2}) = \boldsymbol{0.89}$$

For the morning session (6:00 to 11:00) on April 24, 2012

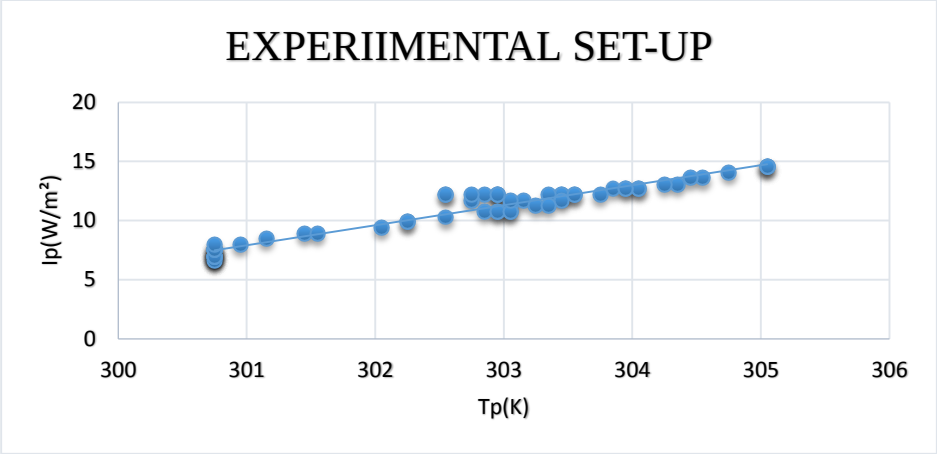

Fig. 4.58: Linear regression analysis of solar radiation (I_p) against temperature (T_p) for the morning session for the experimental set-up recorded on April 24, 2012.

$$\boldsymbol{I_P = 1.6956T_P - 502.47}$$

$$\textbf{Regression Coefficient } (\boldsymbol{R^2}) = \boldsymbol{0.95}$$

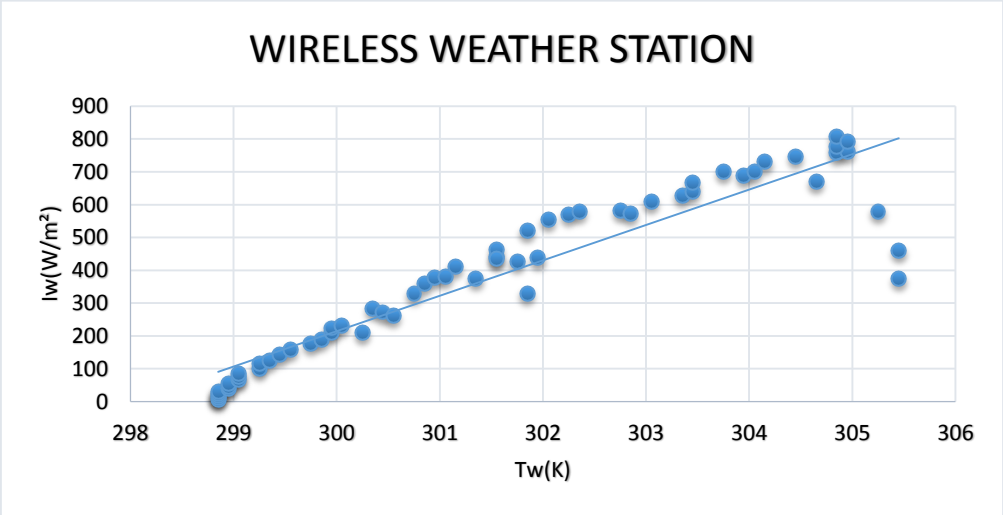

Fig. 4.59: Linear regression analysis of solar radiation (I_w) against temperature (T_w) for the morning session for the wireless weather station recorded on April 24, 2012.

$$\boldsymbol{I_W = 107.88T_W - 32150}$$

$$\textbf{Regression Coefficient } (\boldsymbol{R^2}) = \boldsymbol{0.86}$$

For the evening session (14:00 to 18:00) on April 24, 2012

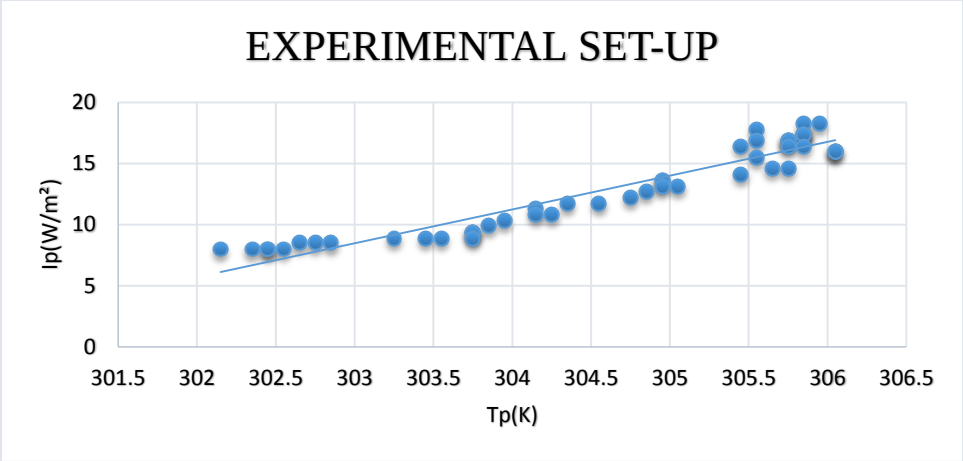

Fig. 4.60: Linear regression analysis of solar radiation (I_p) against temperature (T_p) for the evening session for the experimental set-up recorded on April 24, 2012.

$$\boldsymbol{I_P = 2.7626T_P - 828.6}$$

$$\textbf{Regression Coefficient } (\boldsymbol{R^2}) = \boldsymbol{0.91}$$

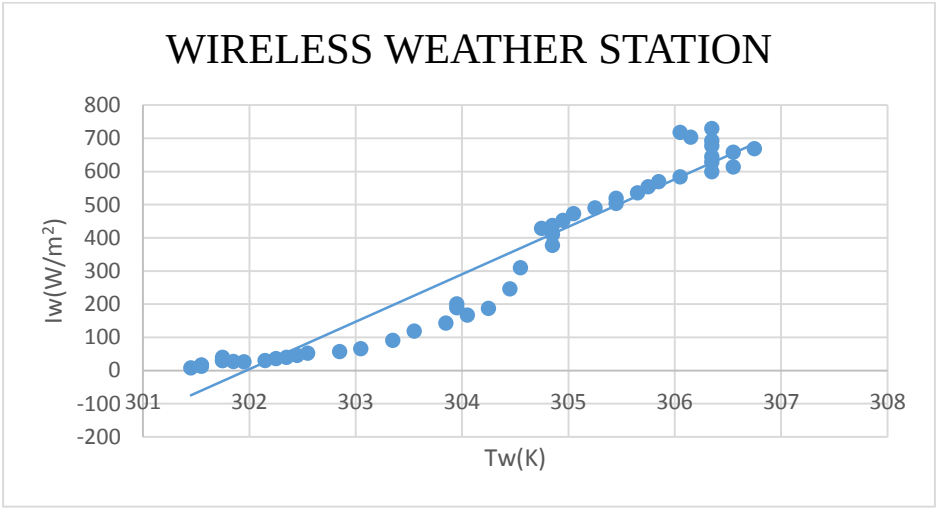

Fig. 4.61: Linear regression analysis of solar radiation (I_w) against temperature (T_w) for the evening session for the wireless weather station recorded on April 24, 2012.

$$\boldsymbol{I_p = 143.12T_p - 43217}$$

$$\textbf{Regression Coefficient } (\boldsymbol{R^2}) = \boldsymbol{0.93}$$

On these two days, 17/4/2012 and 19/4/2012, the weather station did not record any solar radiation activity during the morning session. The data presented here could assess only the evening session of the amount of the solar radiations intercepted. This error could not have happened because of environmental conditions, but could be as a result of system failure of the equipment.

4.3 Correlation between the experimental set-up and the wireless weather station

Comparing the regression coefficient (R^2) values obtained by the ground set up and the wireless weather station, it therefore follows that the experimental set-up had a perfect correlation. The range of the regression coefficient (R^2) values for both the morning and evening sessions obtained from both the ground set-up and the wireless station were; $0.82 - 0.99$ for the morning session for all recorded data days and $0.45 - 0.98$ for the evening session. The wireless weather station also produced the following range of regression coefficient (R^2) values $0.10 - 0.95$ for the morning session and $0.18 - 0.98$ for the evening session. For all the data presented, it could be realized that on the 11/4/2012, both the experimental set-up and the wireless station had R^2value of 0.95 in the morning and different values of R^2 for both the experimental set-up and the weather station in the evenings. The trend can be seen in the following relations; $I_p = 2.3198T_p - 678.14$; $R^2 = 0.95$ and $I_w = 136.22T_w - 40623$; $R^2 = 0.95$ in the morning whiles the evening sessions had $I_p = 2.1098T_p - 625$; $R^2 = 0.81$ and $I_w = 161.31T_w - 48769$; $R^2 = 0.97$.

One observable feature about these two different equations was that, with the experimental set-up, the values of a and b were much lesser than those for the wireless weather station. Despite the difference in the values of a and b, the different set-ups gave a good correlation coefficient in both sessions.

As stated in section 4.1 of this research, due to the position and height of the experimental set-up these differences in the values are likely to occur.

4.4 Correlation between the mean solar radiation (I_m) against mean temperature (T_m)

For a clear and vivid relationship between solar radiation and temperature at the study site, a set of correlation equations were obtained for the entire period. The equations were developed for only the experimental set-up and was split into both morning and evening sessions respectively and is shown below.

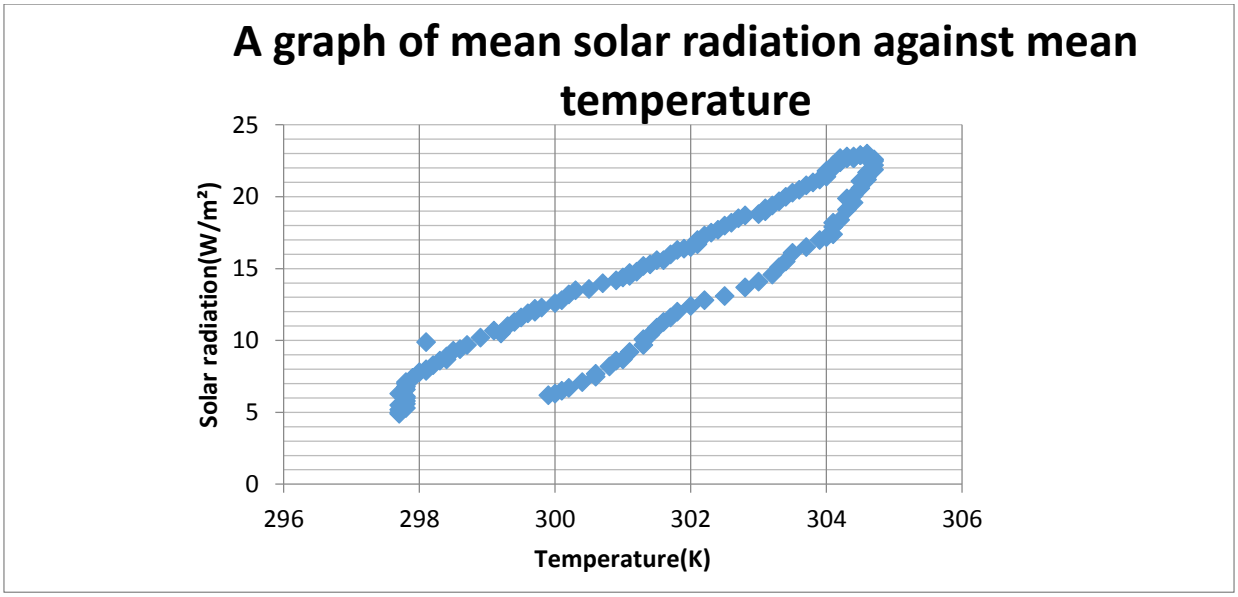

Fig. 4.62: A graph showing the mean solar radiation (I_m) against mean temperature (T_m).

The linear reggresional graphs showing the morning and evening sessions and their obtained equations are also shown below.

Morning session (6:00 to 11:00)

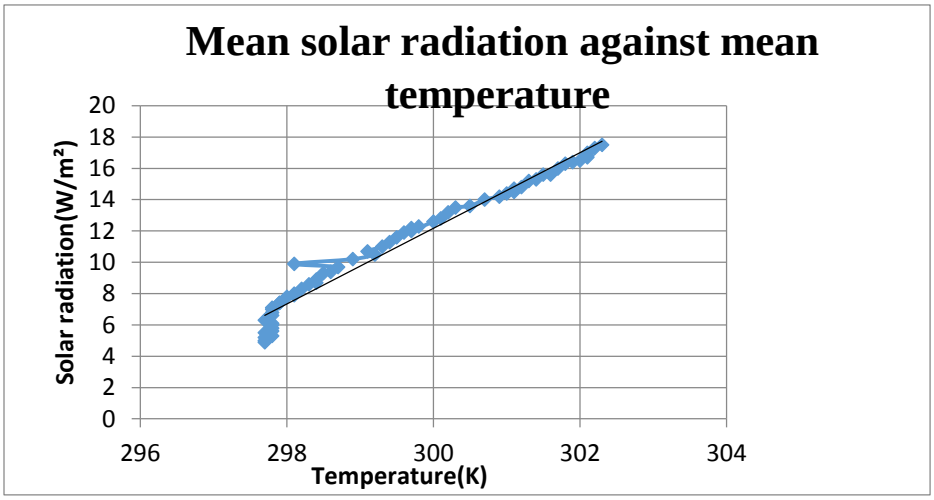

Fig. 4.63: Linear regression analysis of mean solar radiation (I_m) against temperature (T_m) for the morning session obtained for the entire period.

$$\boldsymbol{I_m = 2.417T_m - 713}$$

$$\textbf{Regression Coefficient } (\boldsymbol{R^2}) = \boldsymbol{0.97}$$

Evening session (14:00 to 18:00)

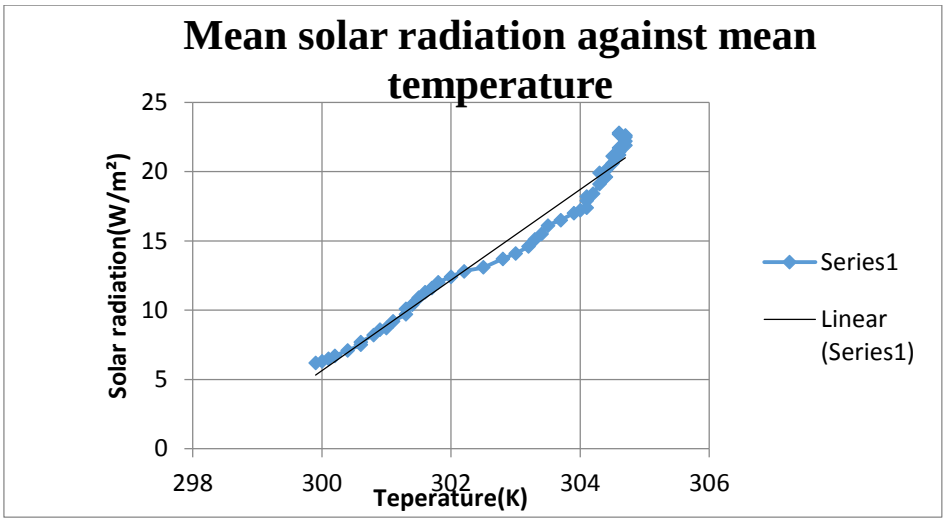

Fig. 4.64: Linear regression analysis of mean solar radiation (I_m) against temperature (T_m) for the evening session obtained for the entire period.

$$\boldsymbol{I_m = 3.265T_m - 974.0}$$

$$\textbf{Regression Coefficient } (\boldsymbol{R^2}) = \boldsymbol{0.97}$$

4.5 Comparing this work with other related works

Preliminary results obtained from this work indicated that as the inception of solar radiation on the earth's surface was high, the temperature increased in that respect and it affected the water holding capacity of the atmosphere. This observation is consistent with results obtained by Medugu *et al*., (2010).

The results from the set-up also indicates that it lags the results from the weather station by a time factor. This can be best explained using the height at which both set-ups were mounted and the obstacles encountered by the inception of the solar radiation. The lag could be seen in the linear regression results obtained by each set-up. The main objective of this work was to correlate the results obtained from the experimental set-up to that of the wireless, and to verify the equations obtained by the experimental set-up. These observations are consistent with those made by Asogwa *et al*., (1995).

CHAPTER FIVE

5.0 CONCLUSION AND SUMMARY

After making a thorough analysis of the solar radiation and the temperature data, the following conclusions can be drawn.

The equations obtained for both the wireless weather station and the experimental set-up gave a very strong correlation for a particular day which was on the 11th April, 2012. The equations obtained for both set-ups for the morning session were; $I_P = 2.3198T_P - 678.14$ and $I_W = 136.22T_W - 40623$ with their Regression Coefficient (R^2) as $R^2 = 0.95$ for the experimental set-up and $R^2 = 0.96$ for the wireless weather station. The set of equations for the evening session for both set-ups were; $I_P = 2.1098T_P - 625$ and $I_W = 161.31T_W - 48769$ with their Regression Coefficient (R^2) values as $R^2 = 0.81$ for the experimental set-up and $R^2 = 0.98$ for the wireless weather station. From these two separate equations, it could be noticed that the temperature and solar radiation for the study area are correlated but lag each other by a time factor. The experimental set-up lags the wireless weather station by a time factor of an hour (1 hr).

To estimate the amount of solar radiation reaching the study area, a mean plot of solar radiation against temperature was obtained for the entire period using the experimental set-up. The plot showed that both temperature and solar radiation were correlated. The equations obtained for the morning session was; $I_m = 2.417T_m - 713$ with a Regression Coefficient (R^2) value of 0.97 and the evening session had $I_m = 3.265T_m - 974.0$ with a Regression Coefficient (R^2) value of 0.97.

The average range within which the pyranometer receives solar radiation at noon was found to be between $20\,W/m^2$ and $25\,W/m^2$. The pyranometer had a low signal responsivity hence the

reason to amplify its signal. These low values could be attributed to the distance at which the set-up was mounted and could also be as a result of environmental factors such as cloud cover. The maximum temperatures recorded during the period showed that the values were obtained between the hours of 12:00 hr local time and 14:00 local hr. The value recorded by the weather station is different from the set-up where values ranging between $869W/m^2$to $965W/m^2$ were observed.

5.1 RECOMMENDATIONS

In view of the abundant amount of energy emitted from the sun in the form of solar radiation, the following recommendations are to be considered:

- An appropriate data logger must be used when replicating this work for manual collection of the data as this will make the solar radiation detection more automatic.
- One year measurement of global solar radiation in the study area should be carried out. This will help to determine the seasonal variation of solar radiation at the particular location.
- A Pyrheliometer should be used simultaneously with a Pyranometer to measure both direct (beam) and global (total) solar radiation. This will help the researcher to determine the amount that is diffused.
- More research activities should be encouraged in the field of solar energy data collection and evaluation in many centers in the country. The solution to the energy crises require an action on proper-coordinated programs especially in the field of solar energy and other alternative energy sources. Accurate data on the availability and nature of the solar energy in a given area is indispensable in this direction.

REFFERENCES

1. Ahrens, C.D. (2006): Meteorology Today: An introduction to weather, climate and environment, 5th Ed, Belmont, California, Brooks Cole.
2. Asogwa, P.U. and Okeke, C.E. (1995): *Design, construction and characterization of local pyranometer for measurement of global radiation*. A paper presented at the international conference on implementation of Renewable energy and Alternative energy technologies, Energy Research Centre, University of Nigeria, Nsuka, Dec, 4-8, 1995.
3. Angstrom, A. (1924): Solar and terrestrial radiation, Q.J.R., Meteorological Society, Vol. 50, pp. 121-126.
4. Badescu, V. (2008): Modelling solar radiation at the Earth's surface, Springer, P.1-3.
5. Baróti, István (1993): Energiafelhasználói Kézikönyv. ["*Manual of energy utilization*"]. Környezettechnika Szolgáltató Kft. Budapest.
6. Battles, F.J., Rubioa, M.A., Tovarb, Olnoc, F.J., and Alados-Alboledos, L. (2000): *Empirical modelling of hourly direct irradiance by means of hourly global irradiance, solar energy*, Vol. 25, pp. 675-688.
7. Bajpai, U. and Kalpana, S. (2009): *Estimation of instant solar radiation by using of instant temperature*, Acta Montanistica Lovaca, Rocnik 14, Vol. 1, P.189-196.
8. Brooks, F.A. (1959): An introduction of Physical microclimatology, Davis, California, P.264, University of California.
9. Bristow, K.N. and Campbell, G.S. (1994): *On the relationship between incoming solar radiation and daily maximum and minimum temperature*, Agric for Meteorology 31, pp. 159-166.

10. Campbell, G.S., and Norman, J.M. (1998): Introduction to Environmental Biophysics, 2nd Ed, New York, Springer-Verlag, pp. 167-183.
11. David, A. and Akpan, U. (2009): *Estimation of horizontal solar radiation in three geographical regions of Ghana*, International conference energy and Meteorology.
12. De-Heer-Amissah, A.N. (1993): *Surface energy budget of some climatic regimes in West Africa*, Ghana Science Journal, Vol. 13(2), pp.103-122.
13. Dickson, K.B. and G. Benneh (1995): A new Geography of Ghana, Longman group, UK.
14. Dimas, F.A.R., Syed, I.G.H, and Mohd, S.A. (2011): *Hourly solar radiation estimation using ambient temperature and relative humidity data*, International Journal of Environmental science and development, Vol. 2(3).
15. Dutton, E.G and J.J Michalsky, T. Stoffel, B.W. Forgan, J. Hickey, T. L. Alberta, I. Reda (2001): *Measurement of broadband diffuse solar irradiance using current commercial instrumentation with a correlation for thermal offset error*, Journal of Atmospheric and Oceanic Technology, 18(3), pp. 297-413.
16. Fredrick, A.K., and Richard, D. (December, 2011): *ICS-UNIDO/EREE training course on GIS mapping in the Ecowas Region*, Renewable Energy Resource in Ghana.
17. Fröhlich, C. and Judith, L. (1998): *The sun's total irradiance: cycles, trends and related climate change uncertainties since 1976*, Geophysical Research Letters, Vol. 25(23), pp. 4377-4380.
18. Fundamentals of Physical Geography, Physical geography.net http://www.physicalgeography.net/fundamentals/image:energy_budget.jpg.
19. Ghana Meteorological Agency (GMA), April 22, 2011.

20. Gueymard, C.A. (2004): *The sun's total and spectral irradiance for solar energy applications and solar radiation models*, solar energy, Vol. 74(6). pp. 423-453.

21. Hanks, R.J. (1992): Applied Soil Physics, Soil water and temperature applications, Springer Verlag, New York.

22. Henderson-Sellers, A. and P.J. Robinson (1994): Contemporary climatology, Longman Scientific and Technical, UK.

23. Jackson, E.A. and Akuffo, F.O. (1992): *Correlation between monthly average daily global irradiation and relative duration of sunshine in Kumasi*, Ghana.

24. Liou, K.N. (2002): An introduction to Atmoshperic Radiation, P.70, 2nd Ed, International Geophysics Series, Volume 84, Elsevier Science (U.S.A).

25. Liu, B.Y. and Jordan, R.C. (1960): *The interrelationship and characteristic distribution of direct, diffuse and total solar radiation*, solar energy, Vol. 4 (3). pp. 1-19.

26. Mcsweeney, C., New, M. and Lizcano, G. (2010): *UNDP climate change country profiles: Ghana.u* http://country-profiles.goeg.ox.ac.uk/[Assessed 10 June, 2011].

27. Medugu, D. W., Burari, F.W and Abdulazeez, A.A. (2010): *Construction of a reliable model pyranometer for irradiance measurements*, African journal of Biotechnology, Vol. 12, pp. 1719-1725.

28. Monteith, J.L. and Unsworth, M. (1973): Principles of Environmental Physics, 2nd Ed, Butterworth-Heinemann Publishing Ltd, reprint 1990, pp. 58.

29. Murry, L.S. (1995): Fundamentals of Atmospheric Physics, Academic Press, New York. pp.649.

30. Muneer, T. (2004): Solar radiation and Daylight models, Elsevier Butterworth-Heinemann, Boston, pp. 390.
31. Myers, D.R., Stoffel T.L, Wilcox, S., Reda, I., Andreas A. (2002): *Recent progress in reducing the uncertainty in and improving pyranometer calibrations*, Journal of Solar Energy Engineering, 124, pp. 44-50.
32. Ötvös, Zoltán: Elpocsékolt energia. (December, 8 200): ["*Waste of energy*"]. Népszabadság, p. 5. (Source: Naplopó Kft.).
33. Salam Abdel, A.S., Higazy, N.A., Veziroglu Nejat, T. (1978): *Solar data application to Egypt, Proceedings of the International Symposium Workshop on Solar energy*, Vol.1. pp. 20-40.
34. Stoffel, T. and Wilcox, S. (2004): *Solar radiation measurements: A workshop for the national association of state universities and land grant colleges, NREL*.
35. Szász, Gábor, Tőkei, László (1997): Meteorológia mezőgazdáknak, kertészeknek, erdészeknek. ["*Meteorology for farmers, gardeners and foresters*"], Mezőgazda Kiadó, Budapest. Vol. 3. Pp. 164-166.
36. Wikipedia, the free encyclopedia http://en-wikipedia.org/wiki/image:electromagnetic_spectrum.jpg.
37. Reindl, D.T., Beckman, W.A., and Duffie, J.A., (1990): *Diffuse Fraction Correlations*, *Solar energy*, Vol. 45. pp. 1-7.
38. World Meteorological Organization (WMO) (1990): *Climate change- A report by a working group of the commission on climatology*, WMO, Geneva.
39. World Meteorological Organization (1983a) '*Measurement of Radiation', Guide to Meteorological Instruments and Methods of Observation*. WMO, Geneva, Vol. 55(9). P. 1-9.